



UNIVERSIDADE ESTADUAL DE MARINGÁ

CENTRO DE CIÊNCIAS AGRÁRIAS

Programa de Pós-Graduação em Ciência de Alimentos

**INATIVAÇÃO FOTODINÂMICA MEDIADA PELOS CORANTES XANTENOS
ROSA BENGALA E EOSINA CONTRA PATÓGENOS DE ORIGEM
ALIMENTAR *Salmonella Typhimurium* E *Staphylococcus aureus***

ADRIELE RODRIGUES DOS SANTOS

MARINGÁ

2019

ADRIELE RODRIGUES DOS SANTOS

**INATIVAÇÃO FOTODINÂMICA MEDIADA PELOS CORANTES XANTENOS
ROSA BENGALA E EOSINA CONTRA PATÓGENOS DE ORIGEM
ALIMENTAR *Salmonella Typhimurium* E *Staphylococcus aureus***

Tese apresentada ao Programa de Pós-Graduação em Ciência de Alimentos da Universidade Estadual de Maringá para a obtenção do grau de Doutora em Ciência de Alimentos.

MARINGÁ

2019

Dados Internacionais de Catalogação-na-Publicação (CIP)
(Biblioteca Central - UEM, Maringá - PR, Brasil)

S237i

Santos, Adriele Rodrigues dos

Inativação fotodinâmica mediada pelos corantes Xantenos, Rosa Bengala e Eosina contra patógenos de origem alimentar *Salmonella Typhimurium* e *Staphylococcus Aureus* / Adriele Rodrigues dos Santos. -- Maringá, PR, 2019.

64 f.: il. color., figs., tabs.

Orientadora: Profa. Dra. Jane Martha Gratin Mikcha.

Tese (Doutorado) - Universidade Estadual de Maringá, Centro de Ciências Agrárias, Departamento de Ciências Agronômicas, Programa de Pós-Graduação em Ciência de Alimentos, 2019.

1. Inativação fotodinâmica. 2. Corantes Xantenos. 3. *Staphylococcus Aureus*. 4. Corante Rosa Bengala. 5. *Salmonella Typhimurium*. I. Mikcha, Jane Martha Gratin, orient. II. Universidade Estadual de Maringá. Centro de Ciências Agrárias. Departamento de Ciências Agronômicas. Programa de Pós-Graduação em Ciência de Alimentos. III. Título.

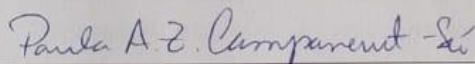
CDD 23.ed. 579.344

Rosana de Souza Costa de Oliveira - 9/1366

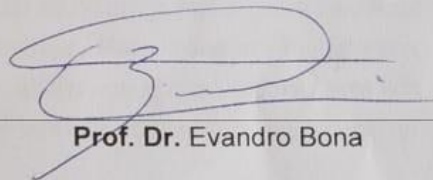
ADRIELE RODRIGUES DOS SANTOS

**“INATIVAÇÃO FOTODINÂMICA MEDIADA PELOS CORANTES XANTENOS
ROSA BENGALA E EOSINA CONTRA PATÓGENOS DE ORIGEM
ALIMENTAR *Salmonella Typhimurium* e *Staphylococcus aureus*”.**

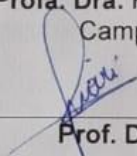
Tese apresentada à Universidade Estadual de Maringá, como parte das exigências do Programa de Pós-graduação em Ciência de Alimentos, para obtenção do grau de Doutor em Ciência de Alimentos.



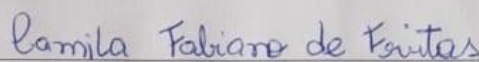
**Profa. Dra. Paula Aline Zanetti
Campanerut-Sá**



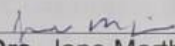
Prof. Dr. Evandro Bona



Prof. Dr. Alex Fiori da Silva



**Profa. Dra. Camila Fabiano de
Freitas**


**Profa. Dra. Jane Martha Gratton Mikcha
Orientadora**

Maringá – 2019

BIOGRAFIA

Adrielle Rodrigues dos Santos nasceu em 1986, na cidade de Campo Mourão – PR. Graduou-se em Tecnologia de Alimentos pela Universidade Tecnológica Federal do Paraná, *campus* Campo Mourão, no ano de 2008 e, especializou-se Vigilância Sanitária de Alimentos pela Universidade Tecnológica Federal do Paraná em 2009. Concluiu, em março de 2014, o mestrado em Ciências de Alimentos, pela Universidade Estadual de Maringá. Trabalhou em Laticínios durante quatro anos e, trabalhou como professora contratada pela Universidade Tecnológica Federal do Paraná, *campus* Campo Mourão, durante dois anos. Atualmente é técnica de laboratório de alimentos da Universidade Tecnológica Federal do Paraná - *campus* Campo Mourão. Tem experiência nas áreas de microbiologia de alimentos, controle de qualidade na indústria de alimentos e tecnologia de leites e derivados.

Dedico

À minha família, em especial meus pais, Hildo e Cilêila, pelo apoio, força, incentivo, companheirismo e amizade. Sem eles nada disso seria possível.

AGRADECIMENTOS

Agradeço primeiramente a DEUS, por estar sempre ao meu lado e conduzir meus passos.

À Universidade Estadual de Maringá e ao Programa de Pós-graduação em Ciência de Alimentos pela oportunidade.

À Universidade Tecnológica Federal do Paraná, por ceder alguns de seus laboratórios para a realização de parte da minha pesquisa.

À Universidade de Aveiro, por me receber e dar suporte para a realização do Doutorado Sanduíche no Exterior.

À professora Dra. Jane Martha Graton Mikcha pela orientação, pela oportunidade e por compartilhar sua experiência.

À professora Dra. Adelaide Almeida, por me receber em seu laboratório na Universidade de Aveiro e compartilhar seus conhecimento e experiência.

Às professoras Dras. Maria da Graça Neves e Amparo Faustino pelos muitos ensinamentos e participarem do processo de aprendizado durante o doutorado sanduíche.

Aos amigos e companheiros de laboratório Alex Fiori, Edinéia Bonin, Daliah Alves Coelho, Andréia Batista pela amizade e por me ajudarem não só nas análises, como também por me escutarem e apoiarem nos momentos de angústia e desânimo.

Aos amigos e companheiros de laboratório Portugueses Marcia Braz, Margarida Lopes, Cristiana Oliveira, Patricia Santos, Catia Vieira, Larindja Pinheiro e, principalmente, Ana Gomes, pela ajuda nas análises e por me receberem e acolherem tão bem.

Às amigas que construí em Portugal, Mônica Cajazeira, Mônica Vasconcelos, Sofia Jewski, Vera Sousa, Luís Pedro Monteiro e Pedro Reis, por se tornarem minha família em Portugal e apoiarem nos momentos de tristeza.

Às amigas que construí nestes anos, que tornaram cada instante muito especial, Leia Andrade, Suelen Siqueira, Maiara Mendes, Vanesa Gesser e Luiz Fernando.

Aos colegas de trabalho na UTFPR Vanessa Rodrigues, Marcos Vieira, Kassia Ayumi, Moacir da Silva, Marcelo Nunes e Jéssica Duca pelo apoio e ajuda.

À minha irmã Gislêine pelo auxílio científico, ao meu cunhado Raphael e à minha sobrinha Giovanna por sempre me divertir nos momentos de crise.

Um agradecimento especial aos meus pais Hildo e Cilêila pelo amor e carinho, pelo exemplo de vida, pelo esforço para que eu chegasse até aqui, pelos conselhos e pelo apoio a cada momento e de todas as formas possíveis.

A todos aqueles que de alguma forma contribuíram para a realização deste trabalho.

MUITO OBRIGADA!

APRESENTAÇÃO

Esta tese de doutorado está apresentada na forma de dois artigos científicos redigidos de acordo com normas de publicação dos periódicos *Journal of Food Safety* (ISSN 1745-4565) and *Antibiotics* (ISSN 2079-6382).

Santos A. R., Silva A. F., de Freitas C. F., da Silva M. V., Bona E., Nakamura C. V., Hioka N., Mikcha J. M. G.. Response Surface Methodology can be used to predict photoinactivation of foodborne pathogens using Rose Bengal excited by 530 nm LED. *Journal of Food Safety*, **2019**.

Santos A. R., Batista A. F. P., Gomes A. T. P. C., Neves M. G. P. M. S., Faustino M. A. F., Almeida A., Hioka N. and Mikcha J. M. G.. The Remarkable Effect of Potassium Iodide in Eosin and Rose Bengal Photodynamic Action against *Salmonella* Typhimurium and *Staphylococcus aureus*. *Antibiotics* **2019**, 8(4), 211; <https://doi.org/10.3390/antibiotics804021>.

GENERAL ABSTRACT

INTRODUCTION. Foodborne diseases are a growing public health problem and are an important cause of morbidity and mortality worldwide. Between 1998 – 2016, in the United States, *Salmonella* spp. was responsible for 2.585 outbreaks of foodborne disease with 8.021 hospitalizations and *Staphylococcus aureus* for 671 outbreaks with 526 hospitalizations. In Brazil, between 2009 – 2018, among the identified agents of foodborne disease, 11.3 % was *Salmonella* spp. and 9.4 % was *S. aureus*, making them two important foodborne pathogens. Preventing outbreaks of foodborne disease requires the control of microorganisms in the food production chain. In this context, an efficient tool for inactivating microorganisms is antimicrobial photodynamic therapy (aPDT), which is a promising and low-price technology effective against a several types of foodborne bacteria. In a PDT, the inactivation of microorganisms is caused by oxidative stress induced by the interaction of a light-excited photosensitizer (PS) in the presence of molecular oxygen. The outcome from the action between PS and visible light is irreversible damage to various molecular constituents of the cells (lipids, proteins, enzymes, and DNA). This technique presents several advantages when compared with the antimicrobials methods, showing to be efficient independently of the antimicrobial resistance profile and to prevent further development of resistance even after several cycles of treatment. Xanthene dyes have been considered good PSs to induce bacterial photoinactivation due to their low price, high molar absorptivity, and high singlet oxygen quantum yield (Φ_{Δ}). The xanthene dyes rose bengal (RB) and eosin Y (EOS) have already proven to be effective against bacteria, however, these dyes showed to be more effective against gram-positive bacteria. This limitation can be overcome using different organic salts such as potassium iodide (KI). Some xanthene dyes are approved for use in drug, cosmetic, and medical applications, and as food additives, while the safety of KI has been reported by Food and Drug Administration (FDA). Several light sources with different wavelengths are available, including the light-emitting diodes (LED). They are becoming a promising alternative to aPDT because of greater flexibility in terms of irradiation time, a wide range of the visible electromagnetic spectrum, including green light (490–570 nm region), and its low price. The mathematical models, as response surface methodology (RSM), can be used to predict the best conditions for inactivating microorganisms by aPDT. These models are valuable tools for applying this technology in the food industry.

34 **AIMS.** The aim of this work was to apply RSM to investigate the antimicrobial photodynamic
35 effect of RB alone against *Salmonella enteric* serotype Typhimurium (ATCC 14028) and
36 *Staphylococcus aureus* (ATCC 25923), as well the combination of the xanthene dyes RB and
37 EOS with the inorganic salt KI against the same bacteria.

38

39 **MATERIAL AND METHODS.** A stock solution of RB and EOS at 1.0 mM and KI at 5 M,
40 prepared in phosphate buffer saline (PBS) pH 7.2 and, a green LED homemade device
41 prototype (10 mW/cm²; 530 ± 40 nm) were used in this work. For the photoinactivation assays
42 500 µL of bacterial suspension (*S. Typhimurium* and *S. aureus*) at 10⁷ CFU/mL with different
43 concentrations of RB or EOS with or without KI were used. Simultaneously, four control groups
44 were included: a positive control; light control (LC); KI control (KIC) and; PS control. After a
45 dark incubation, the samples and the controls LC and KIC were exposed to the green LED light
46 for different irradiation times. Finally, samples were serially diluted in 0.85% saline solution,
47 plated in duplicate onto Tryptic Soy Agar and the CFU/mL was counted. In the first paper it
48 mathematic models were used to investigate the interaction of RB concentration and
49 illumination time in the photoinactivation of *S. Typhimurium* and *S. aureus*. So, for the
50 statistical experimental design, it was used a sequence of designed experiments to model the
51 combined effect of each factor (PS concentration and irradiation time) on the response through
52 mathematical quadratic fitting of the experimental results. A second-order polynomial
53 empirical model describing the relationship between PS concentration and illumination time
54 was developed. It was also performed the PS uptake, as well as the scanning electron
55 microscopy (SEM), transmission electron microscopy (TEM) and flow cytometry. In the
56 second paper it was investigated the use of RB or EOS combined with KI. For this, the same
57 photoinactivation protocol, described above, was used. The photostability and aPDT resistance
58 development assays were also performed.

59

60 **RESULTS AND DISCUSSION.** The derived model used in the first paper predicted the
61 combined influences of PS concentration and illumination time on *S. aureus* and *S.*
62 *Typhimurium* counts, in accordance with predictions and experimental observations ($R^2 =$
63 0.8483 and $p = 0.0013$ for *S. aureus*; $R^2 = 0.9191$ and $p = 0.0001$ for *S. Typhimurium*). Total
64 inhibition of *S. aureus* and *S. Typhimurium* was observed when applying a light dose of 0.125
65 J/cm² and 152.0 J/cm², respectively. The study demonstrates that RB concentrations and
66 illumination times used in the statistical experimental design were generally low, proving the
67 effectiveness of aPDT mediated by RB and green LED light against the microorganisms tested.

68 The application of the RSM showed that the concentration of PS and illumination time are
69 important, but it is necessary to evaluate them separately for each microorganisms to reflect their
70 true influence on the response. *S. aureus* was more susceptible to RB concentration and, the
71 photoinhibitory action increased in a concentration-dependent manner. The illumination time
72 has more influence than PS concentration in the aPDT of *S. Typhimurium*. Bacteria exposed to
73 aPDT lost membrane integrity, as showed by SEM, TEM and flow cytometry. This loss
74 represents significant damage for cells, once multiple functions are linked to the plasma
75 membrane and, a damage in the membrane may lead to cellular content leakage and can cause
76 cell death. To improve the aPDT effect of the xanthene dyes, in the second paper, it was tested
77 the combination of EOS or RB with KI. All PS and KI concentrations tested were able to
78 efficiently inactivate *S. Typhimurium* and *S. aureus*. This combined approach allows a reduction
79 in the PS concentration up to 1000 times, even against one of the most common foodborne
80 pathogens, *S. Typhimurium*, a gram-negative bacterium. Besides, our results showed that there
81 was no significant increase ($p < 0.05$) in resistance of *S. Typhimurium* and *S. aureus* to
82 photosensitization after 10 consecutive sessions of 10 min of irradiation with EOS or RB with
83 KI.

84

85 **CONCLUSIONS.** The use of xanthene dyes in aPDT was able to efficiently inactivate
86 *S. Typhimurium* and *S. aureus*. Applying the RSM in aPDT treatment the photoinhibitory activity
87 could be predict and a new way to use mathematic modeling tools together with aPDT could
88 be provided. So, this approach could be further optimized and applied in food industries.
89 Besides, the addition of KI can strongly potentiate the aPDT mediated by the xanthene
90 derivatives EOS and RB. It was also confirmed that *S. Typhimurium* and *S. aureus* did not
91 develop resistance when submitted to consecutive cycles of aPDT protocol. Therefore, the
92 effective inactivation of both bacteria with low PS concentrations and the low price of the
93 xanthene dyes show that this technology has potential to be easily transposed to the food
94 industry.

95

96 **KEY WORDS:** Inorganic salts; photodynamic inactivation; *Staphylococcus aureus*;
97 *Salmonella Typhimurium*; response surface methodology; xanthene dyes.

98

RESUMO GERAL

99

100

101 **INTRODUÇÃO.** As doenças transmitidas por alimentos são um crescente problema de saúde
102 pública, além de ser uma importante causa de mortalidade em todo o mundo. Entre 1998 - 2016,
103 nos Estados Unidos, *Salmonella* spp. foi responsável por 2585 surtos de doenças transmitidas
104 por alimentos com 8021 hospitalizações e *S. aureus* por 671 surtos com 526 hospitalizações.
105 No Brasil, entre 2009 e 2018, entre os agentes identificados de doenças transmitidas por
106 alimentos, 11.3% eram *Salmonella* spp. e 9.4% eram *S. aureus*, tornando-os dois importantes
107 patógenos de origem alimentar. Prevenir surtos de doenças transmitidas por alimentos requer o
108 controle de microbiano em toda a cadeia de produção de alimentos. Nesse contexto, uma
109 ferramenta eficiente para inativar microrganismos é a terapia fotodinâmica antimicrobiana
110 (TFDa), que é uma tecnologia promissora, de baixo custo e eficaz contra vários tipos de
111 bactérias transmitidas por alimentos. Na TFDa, a inativação microbiana é causada por estresse
112 oxidativo induzido pela interação do fotossensibilizador (FS) excitado pela luz na presença de
113 oxigênio molecular. O resultado é um dano irreversível a vários constituintes moleculares das
114 células (lipídios, proteínas, enzimas e DNA). Essa técnica apresenta várias vantagens quando
115 comparada ao uso de métodos antimicrobianos tradicionais, mostrando ser eficiente
116 independentemente do perfil de resistência antimicrobiana e de impedir o desenvolvimento de
117 resistência, mesmo após vários ciclos de tratamento. Os corantes xantenos têm sido
118 considerados bons FSs para induzir a fotoinativação bacteriana devido ao seu baixo preço, alta
119 capacidade de absorção molar e alto rendimento quântico de oxigênio singlete ($\Phi\Delta$). Os
120 corantes xantenos rosa bengala (RB) e eosina Y (EOS) já provaram ser eficazes contra
121 bactérias, no entanto, esses corantes mostraram-se mais eficazes contra bactérias gram-
122 positivas. Essa limitação pode ser superada pelo uso de diferentes sais orgânicos, como o iodeto
123 de potássio (KI). Alguns corantes xantenos são aprovados para uso em aplicações
124 farmacêuticas, cosméticas e médicas e como aditivos alimentares, enquanto a segurança do KI
125 foi relatada pela *Food and Drug Administration* (FDA). Várias fontes de luz com espectros
126 diferentes estão disponíveis, incluindo os diodos emissores de luz (LED) que estão se tornando
127 uma alternativa promissora para TFDa devido a maior flexibilidade em termos de tempo de
128 irradiação, uma ampla gama de espectro eletromagnético visível, incluindo luz verde (490–570
129 nm) e seu baixo preço. Os modelos matemáticos, como metodologia da superfície de resposta
130 (MSR), podem ser usados para prever as melhores condições para a inativação de
131 microrganismos pela TFDa. Esses modelos são ferramentas valiosas para a aplicação dessa
132 tecnologia na indústria de alimentos.

133

134 **OBJETIVO.** O objetivo deste trabalho foi aplicar a MSR para investigar o efeito fotodinâmico
135 antimicrobiano do RB isoladamente contra *Salmonella enterica* sorotipo Typhimurium (ATCC
136 14028) e *Staphylococcus aureus* (ATCC 25923), bem como a combinação de RB e EOS com
137 o sal inorgânico KI contra as mesmas bactérias.

138

139 **MATERIAIS E MÉTODOS.** Uma solução estoque de RB e EOS a 1,0 mM e KI a 5 M,
140 preparadas em PBS pH 7.2 e um protótipo caseiro de dispositivo de LED verde (10 mW / cm²;
141 530) foram utilizados neste trabalho. Para os ensaios de fotoinativação foram utilizados 500 µL
142 da suspensão bacteriana a 10⁷ UFC / mL com diferentes concentrações de RB ou EOS com ou
143 sem KI. Simultaneamente, quatro grupos controle também foram avaliados: controle positivo;
144 controle de luz (CL); controle de KI (CKI) e; controle do FS. Após incubação no escuro, as
145 amostras e os controles CL e CKI foram expostos ao LED verde por diferentes tempos de
146 irradiação. Finalmente, as amostras foram diluídas em solução salina a 0,85%, semeadas em
147 duplicata em Ágar Tryptic Soy e as UFC / mL foram contadas. No primeiro artigo foram
148 utilizados modelos matemáticos para investigar a interação da concentração de RB e do tempo
149 de irradiação na fotoinativação de *S. Typhimurium* e *S. aureus*. Assim, para o delineamento
150 experimental estatístico, foi utilizada uma sequência de experimentos projetados para modelar
151 o efeito combinado de cada fator (concentração de FS e tempo de irradiação) na resposta, por
152 meio do ajuste quadrático matemático dos resultados. Um modelo empírico polinomial de
153 segunda ordem que descreve a relação entre a concentração de FS e o tempo de iluminação foi
154 desenvolvido. Também foram realizados os ensaios da capturação do FS, microscopia eletrônica
155 de varredura (MEV), microscopia eletrônica de transmissão (MET) e citometria de fluxo. No
156 segundo artigo, investigou-se o uso combinado de RB ou EOS com KI. Para isso, foi utilizado
157 o mesmo protocolo de fotoinativação, descrito acima. Os ensaios de fotoestabilidade e
158 resistência TFDa também foram realizados.

159

160 **RESULTADOS E DISCUSSÃO.** O modelo derivado utilizado no primeiro trabalho previu,
161 as influências combinadas da concentração de FS e do tempo de iluminação nas contagens de
162 *S. aureus* e *S. Typhimurium*, em conformidade com previsões e observações experimentais (R^2
163 = 0,8483 e $p = 0,0013$ para *S. aureus* $R^2 = 0,9191$ e $p = 0,0001$ para *S. Typhimurium*). Foi
164 observada inibição total das células de *S. aureus* e *S. Typhimurium* ao aplicar uma dose de luz
165 de 0,125 J/cm² e 152,0 J/cm², respectivamente. O estudo demonstrou que as concentrações de
166 RB e os tempos de iluminação utilizados no delineamento experimental estatístico para *S.*

167 *aureus* e *S. Typhimurium* foram geralmente baixos, comprovando a eficácia do TFDa mediado
168 por RB e luz verde LED contra esses microorganismos. *S. aureus* foi mais suscetível à
169 concentração de RB e a ação foto inibidora aumentou de maneira dependente da concentração
170 de FS. Enquanto *S. Typhimurium* foi mais suscetível ao tempo de iluminação do que à
171 concentração do FS. As bactérias expostas a TFDa perderam a integridade da membrana, como
172 demonstrado por MEV, MET e citometria de fluxo. Essa perda representa um dano significativo
173 para as células, uma vez que várias funções estão ligadas à membrana plasmática e um dano na
174 membrana pode levar ao vazamento do conteúdo celular, causando a morte celular. Para
175 melhorar a ação da TFDa dos corantes xantenos, no segundo trabalho foram testadas as
176 combinações de EOS ou RB com KI. Todas as concentrações de FS e KI testadas foram capazes
177 de inativar eficientemente *S. Typhimurium* e *S. aureus*. Essa abordagem combinada permitiu
178 uma redução na concentração de FS de até 1000 vezes, mesmo contra um dos patógenos de
179 origem alimentar mais comum, *S. Typhimurium*, uma bactéria gram-negativa. Além disso, os
180 resultados mostraram que não houve aumento significativo ($p < 0,05$) na resistência de *S.*
181 *Typhimurium* e *S. aureus* à fotossensibilização após 10 sessões consecutivas de 10 min de
182 irradiação com a combinação de EOS ou RB com KI.

183

184 **CONCLUSÕES:** O uso dos corantes de xantenos em TFDa foi capaz de inativar
185 eficientemente *S. Typhimurium* e *S. aureus*. Aplicando a MSR no tratamento da TFDa, a
186 atividade foto inibidora pode ser prevista e uma nova maneira de usar ferramentas de
187 modelagem matemática juntamente com aPDT pode ser fornecida. Portanto, essa abordagem
188 pode ser, futuramente, otimizada e aplicada nas indústrias de alimentos. Além disso, a adição
189 de KI potencializou fortemente a TFDa mediada por EOS e RB. Também foi confirmado que
190 *S. Typhimurium* e *S. aureus* não desenvolveram mecanismos de resistência quando submetidos
191 a ciclos consecutivos do protocolo da TFDa. Portanto, a inativação efetiva de ambas as bactérias
192 com baixas concentrações de FS e o baixo preço dos corantes xantenos mostram que essa
193 tecnologia tem potencial para ser facilmente transposta para a indústria de alimentos.

194

195 **PALAVRAS CHAVE.** Corantes xantenos; inativação fotodinâmica; metodologia de superfície
196 de resposta; *Staphylococcus aureus*; sais inorgânicos; *Salmonella Typhimurium*.

197 **Response Surface Methodology can be used to predict photoinactivation of**
198 **foodborne pathogens using Rose Bengal excited by 530 nm LED.**

199

200 **Photoinactivation of pathogens by RB using RSM**

201

202 Adriele Rodrigues dos Santos^{a*}, Alex Fiori da Silva^b, Camila Fabiano de Freitas^c, Marcos Vieira da Silva^d, Evandro
203 Bona^e, Celso Vataru Nakamura^f, Noboru Hioka^g, Jane Martha Gratton Mikcha^h.

204

205 ^aPrograma de Pós-Graduação em Ciência de Alimentos, Universidade Estadual de Maringá, Maringá, PR, Brasil.
206 adrielesantos@hotmail.com.

207 ^bPrograma de Pós-Graduação em Ciência da Saúde, Universidade Estadual de Maringá, Maringá, PR, Brasil.
208 alex_skiba@hotmail.com.

209 ^cPrograma de Pós-Graduação em Química, Universidade Estadual de Maringá, Maringá, PR, Brasil.
210 camila.freitas1989@hotmail.com

211 ^dInstituto Federal de Educação, Ciência e Tecnologia Farroupilha, Alegrete, Rio Grande do Sul, Brasil.
212 marcosvs.83@gmail.com

213 ^eDepartamento de Alimentos, Universidade Tecnológica Federal do Paraná – campus Campo Mourão, Campo Mourão,
214 PR, Brasil. ebona@utfpr.edu.br

215 ^fDepartamento de Ciências Básicas da Saúde, Universidade Estadual de Maringá, Maringá, PR, Brasil.
216 cvnakamura@uem.br

217 ^gDepartamento de Química, Universidade Estadual de Maringá, Maringá, PR, Brasil. nhioka@uem.br

218 ^hDepartamento de Análises Clínicas e Biomedicina, Universidade Estadual de Maringá, Maringá, PR, Brasil.
219 jmgmikcha@uem.br

220

221 *Corresponding Author: Laboratório de microbiologia de alimentos, Departamento de análises clínicas e biomedicina,
222 Universidade Estadual de Maringá, Avenida Colombo, 5790, zona 07, Maringá, 87020-900, PR, Brasil. e-mail:
223 adrielesantos@hotmail.com.

224 <https://orcid.org/0000-0003-3061-6669>

225 **Abstract:** In this work the photodynamic bactericidal effect of Rose Bengal, combined with
226 green LED light, against *S. aureus* and *S. Typhimurium*, was investigated. The interaction of
227 RB concentration and illumination time was evaluated using a response surface methodology,
228 and a second-order polynomial empirical model was adjusted to the experimental data. The
229 derived model predicted the combined influences of these factors on *S. aureus* and *S.*
230 *Typhimurium* counts, in accordance with predictions and experimental observations ($R^2 =$
231 0.8483 and $P = 0.0013$ for *S. aureus*; $R^2 = 0.9191$ and $P = 0.0001$ for *S. Typhimurium*). Total
232 inhibition of *S. aureus* and *S. Typhimurium* was observed when applying a light dose of 0.125
233 J cm^{-2} and 152.0 J cm^{-2} , respectively. The treatments also showed loss of membrane integrity,
234 morphological changes and internal cell structural alterations. In sum, the polynomial model
235 developed could provide accurate information on the combined influences of RB and green
236 LED light in aPDT treatment and, that this combination was able to inactivate *S. aureus* and *S.*
237 *Typhimurium*.

238

239 **Practical applications:** Foodborne diseases are a great public health trouble around the globe
240 and the ingestion of contaminated food represent a substantial risk for millions of people, as
241 well as associated with serious economic consequences for society. However, the common
242 food preservation techniques (chemical preservation; salting, drying, acidification and heat
243 treatment) is related to undesired changes in the nutritional and sensory characteristics of food
244 products. The improvement of new non-thermal technologies that inactivate foodborne
245 pathogens and maintain the cost-effective relation, not causing damage to the environment and
246 microbial resistance is necessary. This study provides an alternative method for foodborne
247 pathogens inactivation the Antimicrobial Photodynamic Therapy (aPDT). Applying the
248 response surface methodology in aPDT treatment the photo inhibitory activity could be predict

249 and a new way to use mathematic modeling tools together with aPDT could be provide and this
250 approach could be further optimized and applied in food industries.

251

252 **Keywords.** *Salmonella* Typhimurium; *Staphylococcus aureus*; RSM; Xanthene dyes;
253 photodynamic inactivation.

254 1. INTRODUCTION

255 Foodborne diseases consist of a broad spectrum of diseases caused by the ingestion
256 of foodstuffs contaminated at any stage in the process (Miller & Cawthorne, 2017). According
257 to the Centers for Disease Control and Prevention (CDC, 2019) between 1998–2016, in the
258 United States, *Salmonella* spp. was responsible for 2,585 outbreaks of foodborne disease with
259 8,021 hospitalizations and *S. aureus* for 671 outbreaks with 526 hospitalizations. In Brazil,
260 between 2009 – 2018, among the identified agents of foodborne disease, 11.3 % was *Salmonella*
261 spp. and 9.4 % was *S. aureus* (Ministério da Saúde, 2019), making them two important
262 foodborne pathogens.

263 Antimicrobial Photodynamic Therapy (aPDT) is an emerging technology that has
264 been shown to be promising and effective against a wide range of foodborne bacteria (Bonin
265 et al., 2018; Hu et al., 2018; Penha et al. 2017; Silva et al., 2018; Tao et al., 2019; Yassunaka
266 et al., 2015). In aPDT, a visible light of a suitable wavelength is used to irradiated a
267 photosensitizer (PS) that, in presence of molecular oxygen, generates reactive oxygen species
268 (ROS) such as hydrogen peroxide (H_2O_2), hydroxyl radical (OH^\cdot), superoxide radical (O_2^\cdot) and
269 singlet oxygen (1O_2), promoting the inactivation of microorganisms (Bartolomeu et al., 2017;
270 Marciel et al., 2018). These cytotoxic species cause oxidative stress and irreversible damage to
271 various biological components of the cell wall (lipids, proteins, enzymes, and DNA) (Martins
272 et al., 2018).

273 Among the substances that could be used as a PS, the anionic water-soluble xanthene
274 dye Rose Bengal (RB) has significant potential in aPDT, cause is an inexpensive PS and its
275 photodynamic mechanism operate largely converting oxygen molecules (O_2) into singlet
276 oxygen (1O_2) upon irradiation with green light (Fadel & Kassab, 2011; Pérez-Laguna et al.,
277 2018; Wen et al., 2017).

278 Several light sources with different spectra are available, including the light-emitting
279 diodes (LED) that are becoming a promising alternative to aPDT because of greater flexibility
280 in terms of irradiation time, a wide range of the visible electromagnetic spectrum, including
281 green light (490–570 nm region) and its low price that could facilitate the study of new
282 compounds for aPDT (Costa et al., 2011; Freire et al., 2014; Peloi et al., 2008).

283 Statistical techniques that can predict the best conditions for inactivating
284 microorganisms by aPDT are valuable tools for applying this technology. One of these
285 techniques is response surface methodology (RSM). It can be used to reduce the number of tests
286 even when studying the effects of several factors at different levels and their influence on each
287 other with a minimum number of tests (Rauf MA, Marzouki N, Körbahti BK. 2008; Zhang et
288 al., 2013).

289 Most of the studies that investigate aPDT mediated by RB use the dye with a modified
290 structure, encapsulated, or added to other compounds (Anju et al., 2018; Gu et al., 2010; Vieira
291 et al., 2018; Wen et al., 2017). In addition, they use fluorescent and halogen lamps instead of a
292 green LED as a source of light (Anju et al., 2018; Cahan R, Schwartz R, Langzam Y & Nitzan
293 Y., 2011; Decraene V, Pratten J & Wilson M. 2006; Gu et al., 2010; Vieira et al., 2018; Wen et
294 al., 2017). To our knowledge, there are no reports of the use of aPDT mediated by RB,
295 combined with green LEDs, against *S. aureus* and *Salmonella* spp. using predictive
296 mathematical models. Hence, the aim of the present study is to evaluate the effects of aPDT
297 using RB excited by 530 nm LED against *Salmonella* Typhimurium and *Staphylococcus*
298 *aureus*, via response surface methodology.

299

2. MATERIALS AND METHODS

2.1. Bacterial strains and culture conditions

Salmonella enterica serotype Typhimurium (ATCC 14028) and *Staphylococcus aureus* (ATCC 25923) were used in this study. The strains were stored at $-20\text{ }^{\circ}\text{C}$ in Brain and Heart Infusion Broth (Difco, Becton Dickinson, Sparks, MD, USA) that contained 20 % (vol/vol) glycerol and, prior to use, they were grown overnight at $37\text{ }^{\circ}\text{C}$ in 5 ml of Tryptic Soy Broth (Difco). Then the microorganisms were harvested by centrifugation at $5000 \times g$ for 4 min, washed three times with 0.85% saline solution. Afterward, the inoculums were adjusted to approximately 1×10^8 colony-forming units (CFU) ml^{-1} using a spectrophotometer at 580 nm (%T 25–30). This standardized suspension was diluted in 0.85% saline solution to approximately 1×10^7 CFU ml^{-1} for use in the experiments (Yassunaka et al., 2015).

2.2. Photosensitizers and LED light source

A stock solution of RB (Sigma Aldrich, Darmstadt, Germany) at 1×10^{-3} μM was prepared in PBS pH 7.2, filter sterilized at a $0.22\text{ }\mu\text{m}$ mixed cellulose esters membrane filter, standardized in a spectrophotometer (UV-Vis Beckman Coulter DU *800) and kept in the dark under refrigeration until use (Bonin et al., 2018).

The green LED homemade device prototype (Figure S1 – supplementary material) has 252 LEDs appropriately arranged on a plate of 13 cm length x 8 cm width, with a distance from the microplate surface of 3.5 cm. The prototype has a fluency rate of 10 mW cm^{-2} and a wavelength of $530 \pm 40\text{ nm}$. The spectral emission of the LEDs system was obtained using a spectrofluorimeter (Varian Cary Eclipse, San Diego, CA, USA). The absolute irradiance of the LEDs was evaluated with a Spectroradiometer USB2000+RAD (Ocean Optics, Winter Park, FL, USA).

324 Light doses (D_{Abs}) and LED beam array of RB at the respective concentrations and
 325 irradiation time were calculated as described by Gerola et al. (2012) and Silva et al. (2018)
 326 (equations 1 and 2), considering the irradiated area of 1.9 cm^2 and the irradiance of 10 mW cm^{-2} .
 327

328

$$329 \quad D_{Abs} = \frac{t}{A} \cdot \int_{\lambda_1}^{\lambda_2} P_{Abs} d\lambda \quad (1)$$

330

331 A is the irradiated area, t is the exposure time, and P_{Abs} was calculated according to the
 332 following equation:

333

$$334 \quad P_{Abs} = X_{Abs} P_{LED \text{ Emitted}} \quad (2)$$

335

336 X_{Abs} is the absorbed light fraction by the PS, P_{Abs} is the absorbed irradiance by the PS,
 337 and $P_{LED \text{ emitted}}$ is the irradiance emitted by LED.

338

339 **2.3.Determination of photoinhibitory activity of rose bengal and green LED light using** 340 **a Statistical Experimental Design**

341 A Rotational Central Composite Design generated by the software Statistica® 8.0
 342 (StatSoft Incorporation, Tulsa, OK, USA, 2007) was used to establish the conditions for the
 343 photoinhibitory activity of RB against *S. Typhimurium* and *S. aureus* (Table 1). The PS
 344 concentrations and illumination times used in the statistical experimental design were pre-
 345 determined in preliminary studies. Twelve experiments, including three replicates of the central
 346 point, were conducted to evaluate the effects of two independent variables: X_1 , the
 347 concentrations of RB (10 to 25 nM, to *S. aureus* and, 10 to 75 μM , to *S. Typhimurium*) and X_2 ,
 348 the illumination time (5 to 15 min for both microorganisms).

349 Table 1. Experimental design with coded and real values of the two independent variables (PS concentration and illumination time) and the light dose values calculated
 350 according to Gerola et al. (2012) and Silva et al. (2018) evaluated for their influence on *S. Typhimurium* and *S. aureus* cell viability.

Experiments	Coded values		<i>S. aureus</i>				<i>S. Typhimurium</i>			
	X ₁	X ₂	Real values				Real values			
			Concentration (nM)	Time (min)	Light Doses (J cm ⁻²)	Cell viability (Log CFU ml ⁻¹) [†]	Concentration (μM)	Time (min)	Light Doses (J cm ⁻²)	Cell viability (Log CFU ml ⁻¹) [†]
Control (PS-L-) [‡]	---	---	0	0	0	5.49 ±0.05	0	0	0	7.34 ±0.03
1	-1.00000	-1.00000	12.00	5	0.029	3.99 ±0.23	11.80	6.5	26.900	6.73 ±0.17
2	-1.00000	1.00000	12.00	15	0.086	2.10 ±1.13	11.80	13.5	55.900	3.21 ±0.33
3	1.00000	-1.00000	24.00	5	0.057	2.98 ±0.37	64.20	6.5	73.200	4.11 ±0.32
4	1.00000	1.00000	24.00	15	0.172	1.40 ±0.82	64.20	13.5	152.000	Bql [§]
5	-1.41421	0.00000	9.50	10	0.046	4.11 ±0.28	9.47	10	35.100	7.26 ±0.16
6	1.41421	0.00000	26.50	10	0.125	Bql [§]	75.05	10	120.000	1.77 ±0.99
7	0.00000	-1.41421	18.00	3	0.027	4.09 ±0.22	38.00	5.05	44.000	5.73 ±0.15
8	0.00000	1.41421	18.00	17	0.155	1.77 ±0.99	38.00	14.95	130.200	0.92 ±0.69
9	0.00000	0.00000	18.00	10	0.091	3.12 ±0.81	38.00	10	87.100	1.40 ±0.93
10	0.00000	0.00000	18.00	10	0.091	3.43 ±0.17	38.00	10	87.100	2.00 ±0.24
11	0.00000	0.00000	18.00	10	0.091	2.56 ±1.11	38.00	10	87.100	3.69 ±0.25
12	0.00000	0.00000	18.00	10	0.091	3.30 ±0.18	38.00	10	87.100	2.24 ±0.97

351 [†]Values are mean followed by standard deviation

352 [‡]Positive control, containing only the inoculum in PBS and without illumination.

353 [§]Bql - below the quantification limit of 2 log CFU mL⁻¹.

354 In a 24-well microplate, an aliquot of 25 μL of bacterial suspension at 1×10^7 CFU mL^{-1}
 355 ¹ was homogenized with 475 μL of RB at different concentrations and kept in the dark for 10
 356 min. After incubation, the microplate was illuminated with a green LED light (PS+L+) up to
 357 the maximum time of 15 min. Three controls were also evaluated: PS control, containing the
 358 inoculum and PS without illumination (PS+L-); light control, containing only the inoculum in
 359 PBS under illumination (PS-L+), and; the positive control, containing only the inoculum in PBS
 360 and without illumination (PS-L-).

361 After photoinactivation treatment, the samples were diluted in 0.85 % saline solution,
 362 10 μL droplets of each dilution were plated on Trypticase Soy Agar (Difco) plates in order to
 363 determine the number of culturable cells (CFU mL^{-1}). The plates were incubated at 37 °C for
 364 24 h and the CFU were counted (Bonin et al., 2018).

365

366 **2.4.Statistical analysis**

367 A second-order polynomial model was used for fitting the experimental data and its
 368 coefficients were obtained by multiple linear regression (Equation 3).

369

$$370 \hat{Y} = b_0 + b_1X_1 + b_2X_2 + b_{11}X_1^2 + b_{22}X_2^2 + b_{12}X_1X_2 \quad (3)$$

371

372 Where \hat{Y} is the predicted response; b_0 is the regression coefficient for the intercept; b_1
 373 and b_2 are the regression coefficients representing the linear effect terms; b_{11} and b_{22} are the
 374 quadratic effect terms; b_{12} is the interaction effect terms; and X_1 and X_2 are the independent
 375 variables in coded values. A t-test was performed for analyzing the regression coefficients and
 376 excluding those that were not significant ($p > 0.05$) to the mathematical models. The models
 377 were considered significant for the prediction of the responses via the determination of the
 378 coefficients of determination (R^2), the adjusted coefficients of determination (R^2_{adj}), and the

379 ANOVA ($p < 0.05$). The mean square error (MSE) was also used as residual analysis of the
380 model. The software Statistica® 13 (TIBCO Software Inc, 2017) was used for the statistical
381 analysis described above and for generating the response surface plots.

382

383 **2.5. Rose bengal uptake**

384 Bacterial suspensions, prepared according Manoil D, Filieri A, Schrenzel J &
385 Bouillaguet S. (2016) with modifications, in the presence of different concentrations of RB
386 (Table 1), were incubated at room temperature in the dark for 10 min. Control and treated
387 samples were harvested by centrifugation at 9.500 x g for 5 min and washed thrice with 0.85%
388 saline solution. To extract RB incorporated into cells, the bacterial pellet was dissolved in 99.9
389 % DMSO, sonicated (10 min at 35 kHz, Sonorex, Bandelin electronics, Berlin, DE). The
390 samples were transferred into a quartz cuvette and measured fluorescence emission in a
391 spectrofluorimeter (Varian Cary-Eclipse). Lysed bacteria in DMSO, without RB, were used as
392 blanks. A calibration curve of fluorescence emission of RB versus concentration, in DMSO,
393 was used to determine the concentration of RB in samples. Experiments were performed in
394 triplicate and repeated three times.

395

396 **2.6. Scanning electron microscopy**

397 Sample preparation was performed according Bonin et al. (2018). Control and treated
398 bacteria were fixed with 2.5 % glutaraldehyde (Sigma-Aldrich, Louis, MO, USA) in 0.1 M
399 cacodylate (SEM, Hatfield, PA, USA) at 4 °C for 2 h. Then the samples were centrifuged,
400 washed thrice in the same buffer, and placed in coverslips containing poly-L-lysine for one
401 hour. The coverslips were washed with cacodylate buffer and dehydrated using increasing
402 concentrations of ethanol (50, 70, 80, 90, and 100 %). They were submitted to CO₂ critical-

403 point-dried and covered with gold. The samples were observed in a QUANTA 250 scanning
404 electron microscope (FEI, Amsterdam, Netherlands).

405

406 **2.7. Transmission electron microscopy**

407 Sample preparation was performed according to Jiang et al. (2013) with modifications.
408 After photodynamic treatment, control and treated bacteria were fixed with 2 % glutaraldehyde
409 in 0.1 M cacodylate for one day. After fixation, the samples were centrifuged, washed thrice
410 with cacodylate buffer, and post fixed with 1 % osmium tetroxide for one hour. Then, the cells
411 were dehydrated in graded acetone and embedded in Epon 812 (Electron Microscopy Sciences,
412 Fort Washington, PA), so the ultrathin sections (80 to 100 nm) were prepared, stained with
413 uranyl acetate and lead citrate. The observation of the ultrastructure of the samples was in an
414 electron transmission microscope (JEM-1400; Jeol, USA).

415

416 **2.8. Flow cytometry**

417 Flow cytometry was performed according Bonin et al. (2018) using the LIVE/DEAD
418 BacLight Bacterial Viability and Counting Kit (L34856), (Molecular PROBES, Oregon, USA).
419 Treated bacteria, positive control (PS-L-) and negative control were centrifuged at 10.000 x g
420 for 3 min and resuspended in 1 mL of 0.85 % saline solution. Subsequently, were added to the
421 samples 1.5 µL of propidium iodide (PI) and 1.5 µL of SYTO 9, then the samples were kept in
422 the dark for 15 min. The stained samples were analyzed on a flow cytometer (BD Fasca Canto
423 II).

424

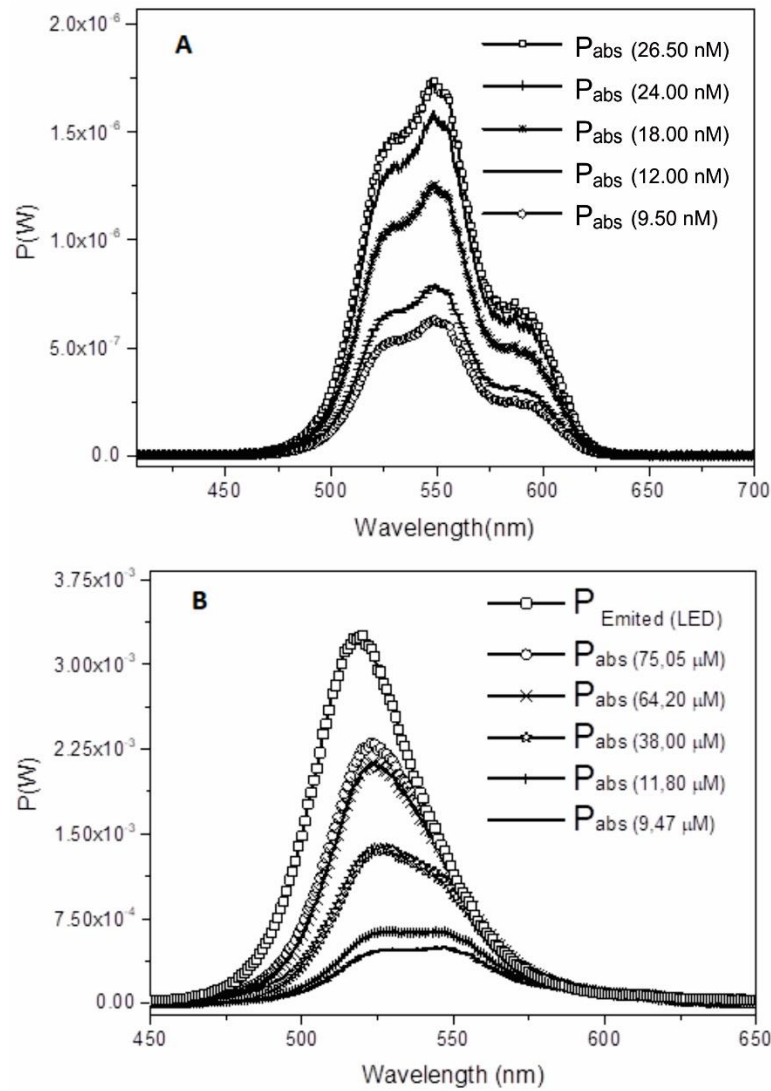
425

426 **3. RESULTS**

427 **3.1.Light doses**

428 In this study, the absorbed potency (P_{Abs}) and the light doses (D_{Abs}) were calculated as
 429 previously described (Gerola et al., 2012; Silva et al., 2018). It was necessary to explaining the
 430 exact fraction of the LED power (P_{Emit}) that was absorbed by the different concentrations of the
 431 PS in varying illumination times, as shown in Table 1. It is also possible to observe that the
 432 intensities of the RB spectral profiles are directly proportional to the dye concentrations (Fig.
 433 1) and, consequently, the light doses increase as the PS concentrations are higher.

434



435

436 Fig. 1 - Spectra of light emitted by LED ($P_{LED\text{ Emitted}}$) and power absorbed by RB (P_{Abs}) in different concentrations
 437 for *S. aureus* (A), (—□— 26.50 nM; —+— 24.00 nM; —*— 18.00 nM; ——— 12.00 nM;
 438 —○— 9.50 nM) and *S. Typhimurium* (B), (—○— 75.05 μ M; —×— 64.20 μ M; —*— 38.00 μ M;
 439 —+— 11.80 μ M; ——— 9.47 μ M). Potency (Watt); wavelength (nm).

440

441 The complete inhibition of *S. Typhimurium* was observed at 64.20 μ M and an
 442 illumination time of 13.5 min (152 J cm^{-2}), as shown in Table 1. However, with a small increase
 443 in the illumination time (14.95 min.) and just over half of the PS concentration (38 μ M), it was
 444 possible to observe more than 6 log CFU mL^{-1} of reduction in the bacterial viability.
 445 Maintaining the PS concentration (38 μ M) and decreasing the illumination time to ten minutes,
 446 we still obtained approximately 4 log CFU mL^{-1} of reduction in the viability of *S. Typhimurium*.

447

448 Table 2. Regression coefficients of the full mathematical model to predict the photoinhibitory effects of RB and
 449 green LED light against *S. Typhimurium* and *S. aureus*.

Coefficient [†]	<i>Staphylococcus aureus</i>		<i>Salmonella Typhimurium</i>	
	Regression	P-value	Regression	P-value
	coefficient		coefficient	
b ₀	3.0578	0.0001	2.3316	0.0010
b ₁	- 0.9405	0.0066	- 1.6994	0.0009
b ₁₁	- 0.4927	0.1057	0.9873	0.0193
b ₂	- 0.8455	0.0107	- 1.8039	0.0006
b ₂₂	- 0.0555	0.8374	0.3951	0.2516
b ₁₂	0.0781	0.8194	- 0.1481	0.7200

450 [†]b₀ – intercept; b₁ – linear coefficient of PS concentration; b₂ – linear coefficient of illumination time; b₁₁
 451 – quadratic coefficient of PS concentration; b₂₂ – quadratic coefficient of illumination time; b₁₂ - interaction
 452 coefficient between PS concentration and illumination time.

453 In the mathematical models, only significant coefficients ($p < 0.05$) were considered
454 (Table 2). Although the quadratic coefficient of PS concentration (b_{11}) was not significant, it
455 was considered in the composition of the mathematical model for *S. aureus*, since the model
456 evaluation were better with it, that is, by keeping this coefficient the adjusted R² increases and
457 the residual variance decreases.

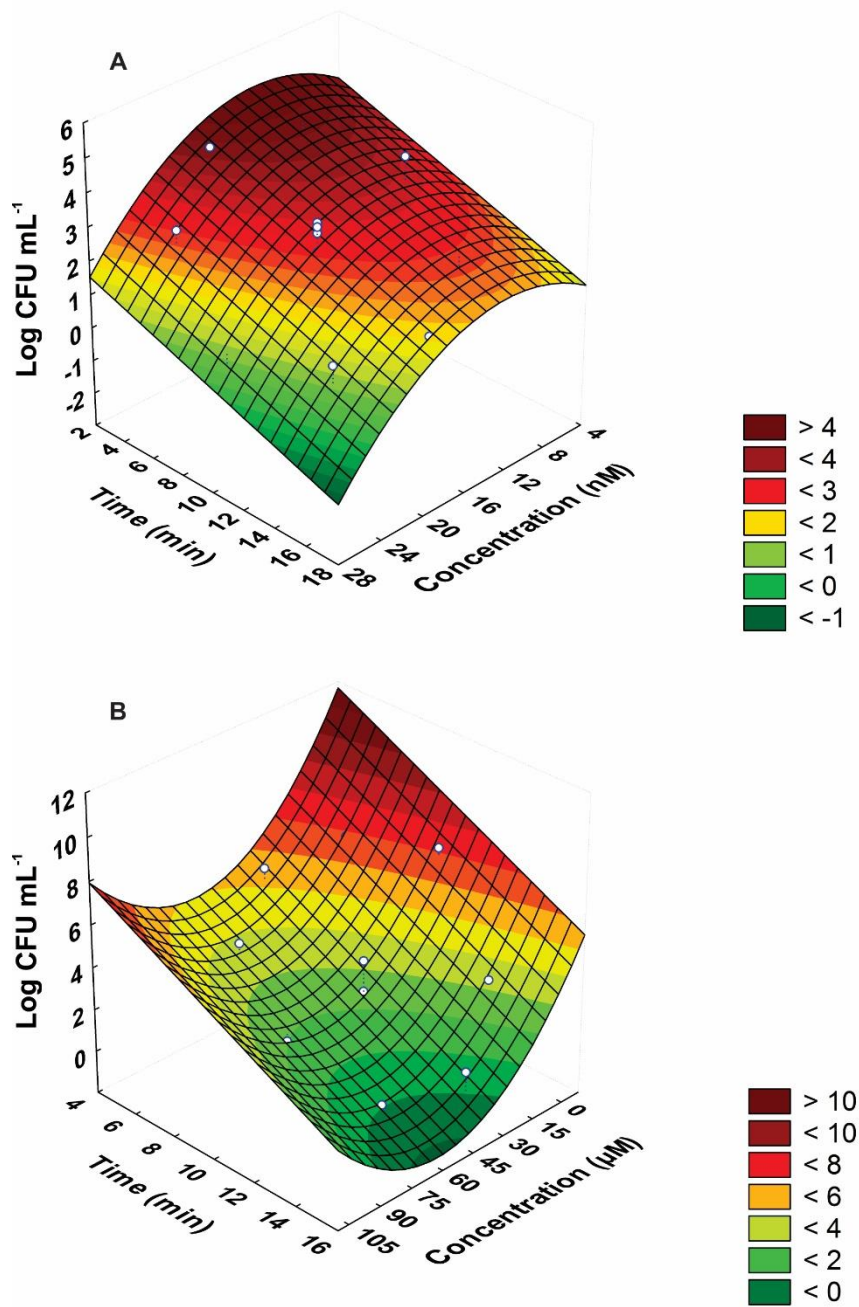
458 The analysis of variance (ANOVA), showed at table S1, demonstrates that the models
459 are significant for both microorganisms (*S. aureus*, $p = 0.0013$; *S. Typhimurium* $p = 0.0001$)
460 and did not show lack of fit (*S. aureus*, $p = 0.196$; *S. Typhimurium* $p = 0.8161$). The R²_{adj} value
461 (0.7879 for *S. aureus* and 0.8887 for *S. Typhimurium*) being the measure of the goodness of fit
462 of the model, indicates that 78.79 % (for *S. aureus*) and 88.87 % (for *S. Typhimurium*) of the
463 total variation is explained by the model. The MSE was 0.2181 for *S. aureus* and 0.4009 for *S.*
464 *Typhimurium*. Considering the R²_{adj}, MSE, the significance of prediction, lack of fit of these
465 models, and the natural variability related to the microbiological experimentation (Doria Filho,
466 2001), the models were considered adequate for predicting the photo inhibitory activity of RB
467 with green LED light.

468 In Table 2, it is possible to observe that the models showed no significant interactions
469 between PS concentration and illumination time (b_{12}) ($p > 0.05$), for both *S. aureus* and *S.*
470 *Typhimurium*. The regression coefficients of the mathematical models showed that the
471 quadratic effect for the variable illumination time (b_{22}) was not significant either ($p > 0.05$), for
472 both bacteria.

473 For the *S. aureus* model, the ANOVA, table S2, showed that the variables PS
474 concentration and illumination time exhibited linear negative effects (Table 2 and Fig 2A); in
475 other words, as PS concentration or illumination time increases, there is a tendency to decrease
476 the bacterial counts. However, the linear effect of the PS concentration was the most significant,
477 demonstrating that PS concentration has a greater influence than illumination time in reducing

478 *S. aureus* counts. Even the quadratic effect of the PS concentration variable was not significant
479 but was considered in the composition of the *S. aureus* mathematical model and indicated that
480 the PS concentration has a low photo inhibitory effect until approximately 6.00 nM (Fig 2A).
481 However, the photo inhibitory effect was pronounced when PS concentration was higher than
482 10.00 nM (Fig 2A).

483 For the *S. Typhimurium* model, the ANOVA (Table S2 – supplementary material)
484 showed that the linear negative effect of illumination time was the most significant, followed
485 by the linear negative effect of PS concentration, similar to *S. aureus*. These results also
486 demonstrate that the time of exposure to light has higher influence than the concentration of
487 RB in *S. Typhimurium* photoinactivation. The less significant effect was the quadratic positive
488 of PS concentration, which indicated that the increase of PS concentration promotes a decrease
489 in the bacterial count; however, from approximately 65 μ M (Fig 2B), this term begins to show
490 a decrease in its inhibitory effect.



491

492 Fig. 2 – Response surface describing interactive influence of the two independent factors tested: PS concentration

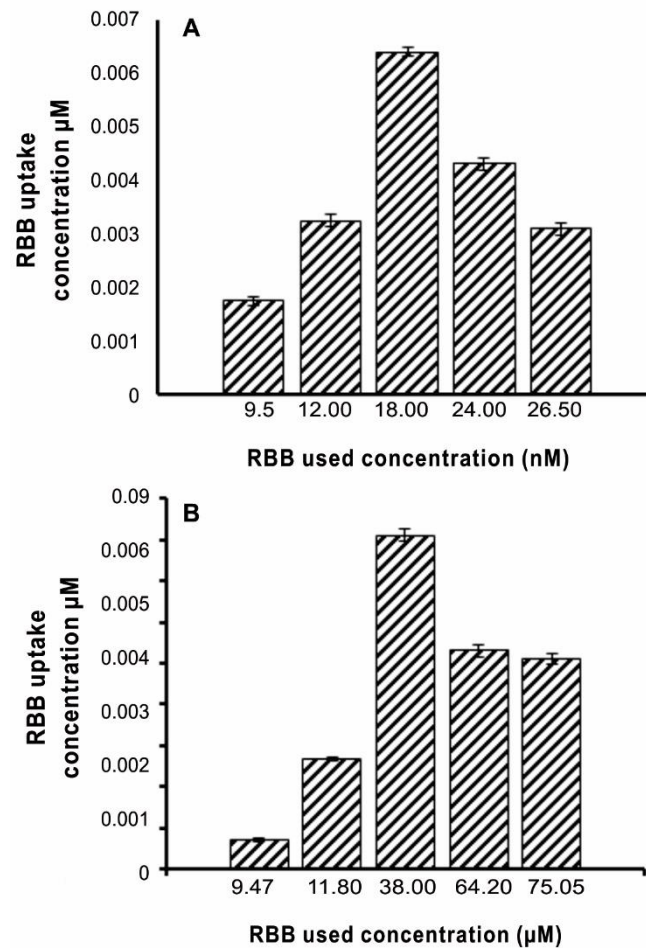
493 and illumination time for *S. aureus* (A) and *S. Typhimurium* (B) counts (■ > 4 log CFU ml⁻¹; ■ < 4 log CFU494 ml⁻¹; ■ < 3 log CFU ml⁻¹; ■ < 2 log CFU ml⁻¹; ■ < 1 log CFU ml⁻¹; ■ < 0 log CFU ml⁻¹).

495

496 **3.2. Rose bengal uptake**497 Figure 3 shows that both *S. aureus* and *S. Typhimurium* immobilized the photosensitizer498 after 10 min incubation. When the concentration of RB was increased up to 18 nM for *S. aureus*

499 and 38 μM for *S. Typhimurium*, it was possible to observe an increase in the PS uptake in a
 500 dependent manner. However, when RB concentration was increased, above those already
 501 mentioned, the uptake showed decay for both strains.

502



503

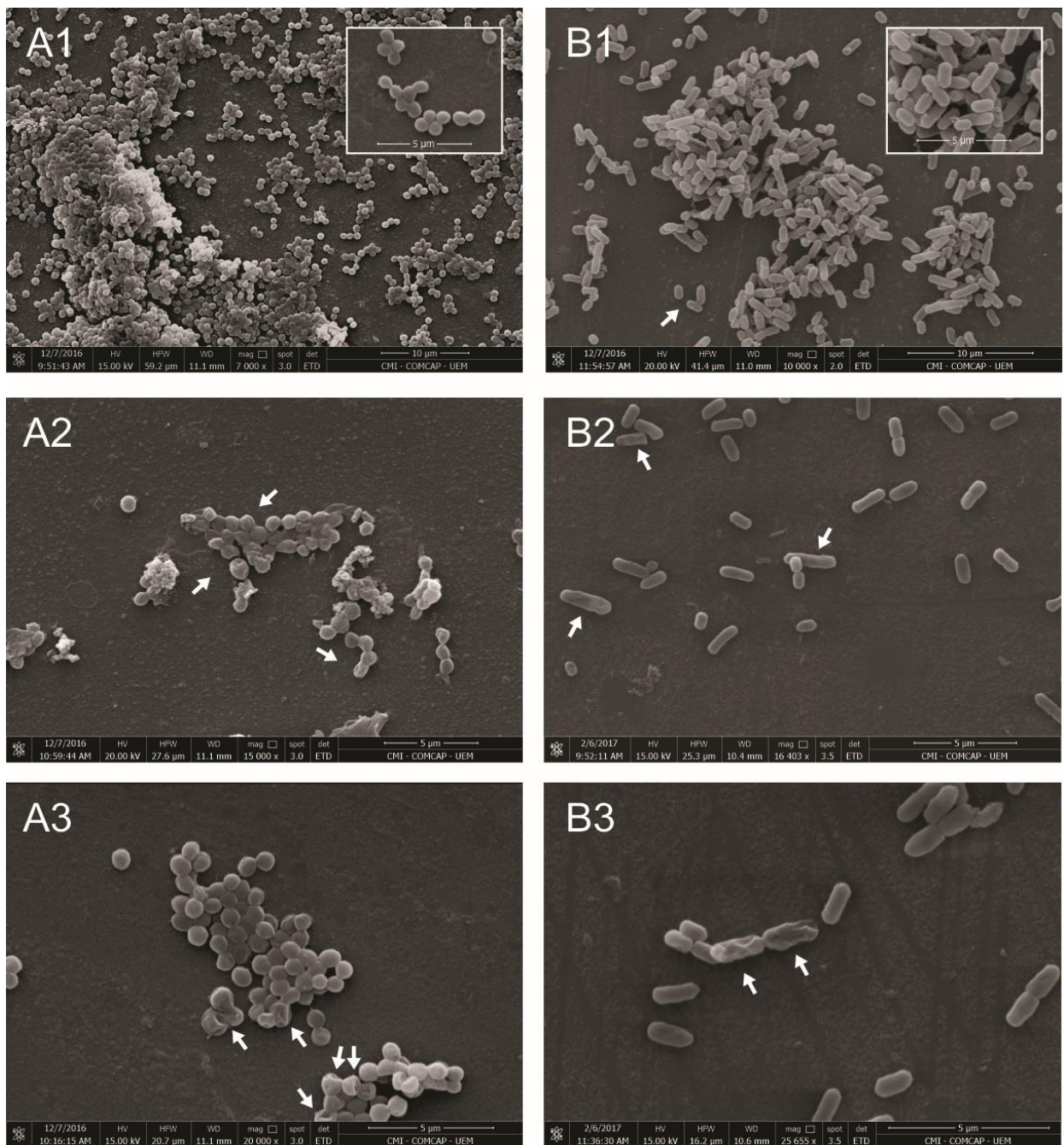
504 Fig. 3 – Rose Bengal uptake by *S. aureus* (A) and *S. Typhimurium* (B): concentration of RB extracted after 10 min
 505 incubation.

506

507 3.3.Scanning electron microscopy

508 The morphological alterations of *S. aureus* (Fig. 4A) and *S. Typhimurium* (Fig. 4B)
 509 induced by RB at 24.00 nM and 64.20 μM illuminated for 5 and 6.5 min, respectively, were
 510 evaluated by SEM. Positive control (PS-L-) was with its characteristic morphology and had a
 511 uniform and smooth cell surface (Fig 4 – A1 and B1), while the photoinactivated cells (Fig 4 –

512 A2, A3, B2 and B3) showed their cell membrane and morphology with distortions, appearing
 513 wrinkled and withered.



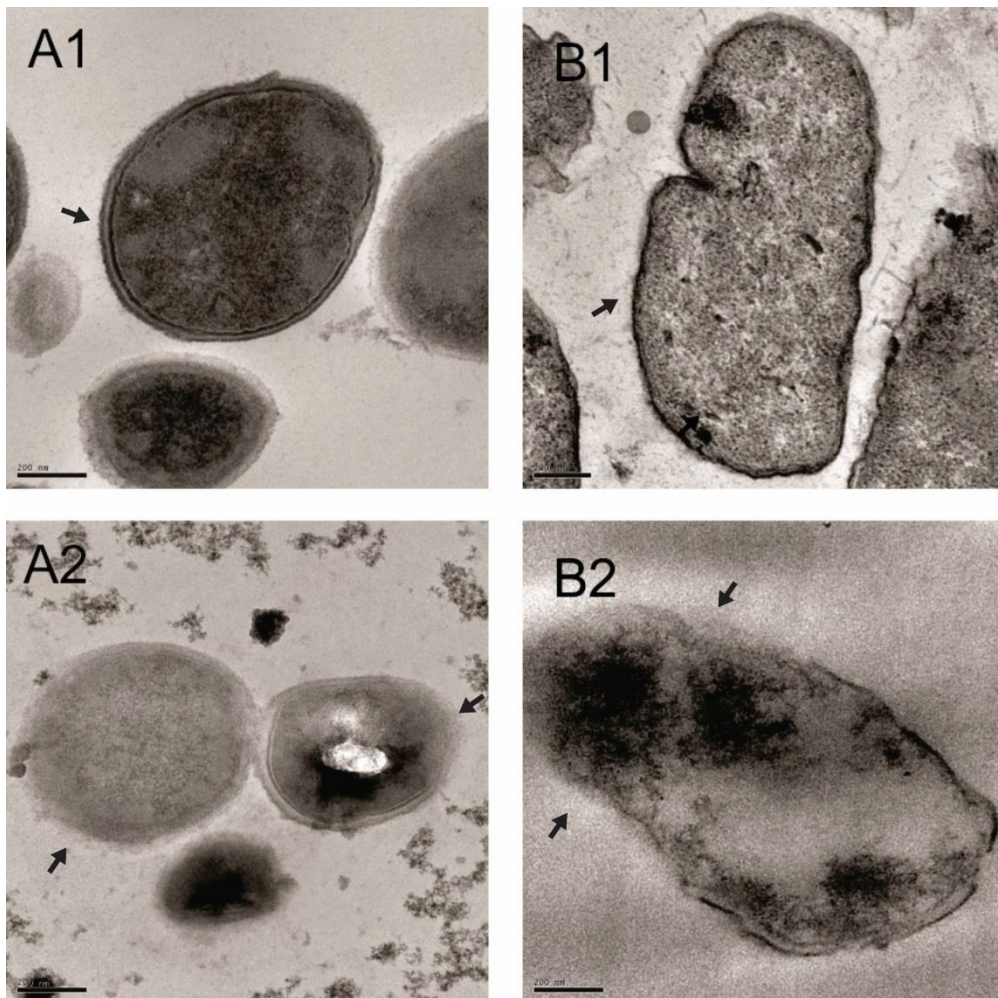
514

515 Fig. 4 – Scanning electron microscopy of *S. aureus* (A), positive control (PS-L-) (A1 - magnification
 516 7.000x), bacteria treated with 24.00 nM of RB and 5 min of illumination (A2 - magnification 15.000x and A3 -
 517 magnification 20.000x) and; *S. Typhimurium* (B), positive control (PS-L-) (B1 - magnification 10.000x), bacteria
 518 treated with 64.20 μ M of RB and 6.5 min of illumination (B2 - magnification 16.403x and B3 - magnification
 519 25.655x).

520

521 **3.4. Transmission electron microscopy**

522 The ultrastructural morphology of *S. aureus* (Fig. 5A) and *S. Typhimurium* (Fig. 5B)
523 induced by RB at 24.00 μ M and 64.20 μ M illuminated for 5 and 6.5 min, respectively, were
524 observed using TEM. The *S. aureus* control cells presented normal and spherical morphology,
525 with dense and homogeneous cytoplasm and intact cell walls and membranes (Fig. 5 – A1). In
526 contrast, treated cells appeared to have undergone lysis, with damaged cell walls and
527 membranes, resulting in leakage of cellular contents with translucent cytoplasm (Fig. 5 – A2).
528 The *S. Typhimurium* cells in the control group had a densely stained cytoplasm and were in a
529 shape of a rod (Fig. 5 - B1). In contrast, the cells in the treatment group showed that the
530 cytoplasm was damaged and leaking, with loss of structural integrity of the membrane and cell
531 wall also being observed, as evident in Fig. 5 – B2).



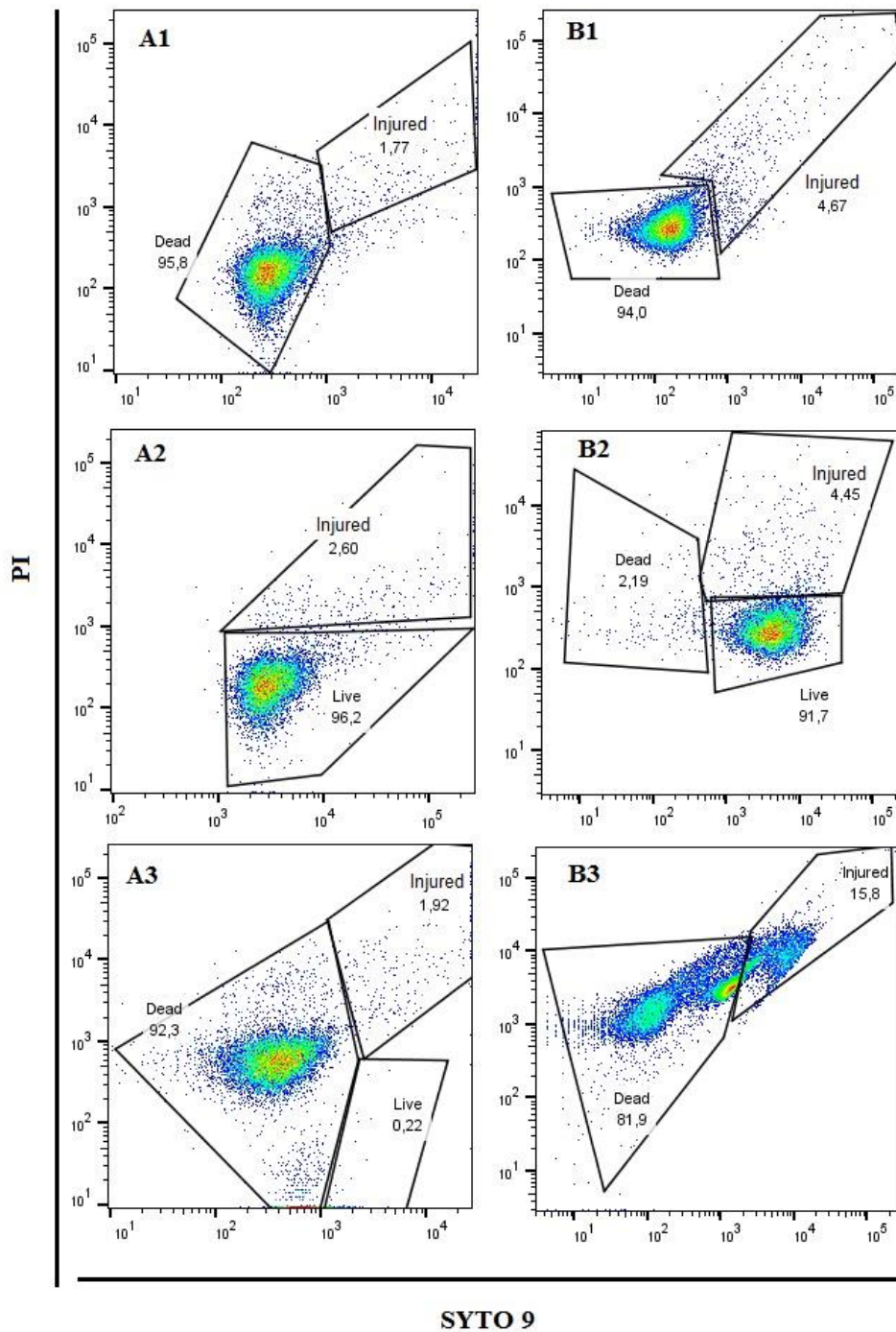
532

533 Fig. 5 – Transmission electron microscopy of *S. aureus* (A), positive control (PS-L-) (A1), bacteria treated with
534 24.00 nM of RB and 5 min of illumination (A2) and; *S. Typhimurium* (B), positive control (PS-L-) (B1), bacteria
535 treated with 64.20 μ M of RB and 6.5 min of illumination (B2). Bar represent 200 nm.

536

537 **3.5.Flow cytometry**

538 The detection of different subpopulations based on the membrane integrity of *S. aureus*
539 and *S. Typhimurium* are shown in Figure 6. The negative control (bacteria death with isopropyl
540 alcohol) exhibited, for *S. aureus*, 95.8 % of dead cells and 1.77 % of injured cells (Fig. 6 – A1),
541 while *S. Typhimurium* showed 94.0 % of dead cells and 4.67 % of injured cells (Fig. 6 – B1).
542 The positive control (PS-L-) showed that 96.2 % of the *S. aureus* cells showed up positive for
543 SYTO 9 with a strong green fluorescence, indicating the integrity of the membrane. Already,
544 2.60 % of the *S. aureus* cells showed double-staining, indicating that the cells were injured (Fig.
545 6 – A2). For *S. Typhimurium*, the positive control (PS-L-) showed 91.7 % of live cells, 4.45 %
546 of injured cells, and 2.19 % of dead cells (Fig 6 - B2).



547

548 Fig. 6 - Flow cytometric analysis of *S. aureus* (left side): negative control (bacteria with isopropyl alcohol) (A1),
 549 positive control (PS-L-) (A2), bacteria treated with 24.00 nM of RB and 15 min of illumination (A3); and of *S.*
 550 *Typhimurium* (right side): negative control (bacteria with isopropyl alcohol) (B1), positive control (PS-L-) (B2),
 551 bacteria treated with 38.00 μ M of RB and 14.95 min of illumination, stained with SYTO 9 and PI. SYTO 9
 552 fluorescence on the X-axis plotted against PI fluorescence on the Y-axis. Numbers in each gate represent the
 553 percentage of events.

554

555 When *S. aureus* was exposed to 24.00 nM of RB and 15 min of illumination, 92.3 %
556 dead cells, 1.92 % injured cells, and 0.22 % live cells were obtained (Fig. 6 – B3). After
557 exposure to 38.00 µM of RB and 14.95 min of illumination, *S. Typhimurium* showed 81.9 %
558 dead cells and 15.87 % injured cells, as shown in Fig 6 – B3.

559

560 **7. Discussion**

561 aPDT is a novel, emerging technology that may be particularly useful in increasing
562 microbial food control, with significant advantages over conventional methods (Luksiene &
563 Brovko, 2013). Some authors showed good results in eliminate foodborne pathogens and food
564 spoilage microorganisms in meat and seafood (Liu et al., 2016; López-Carballo Hernández-
565 Muñoz, Gavara & Ocio, 2008; Wu et al., 2016) in extend the shelf-life and improve
566 microbiological quality of fruits (Al-Asmari, Mereddy & Sultanbawa, 2018; Tao et al., 2019)
567 and in decontaminate packing surfaces (Luksiene, Buchovec & Paskeviciute, 2009; Luksiene
568 & Paskeviciute, 2011). However, it is necessary to say that the most researches obtained its
569 results from experiments in a laboratory scale (Silva et al., 2018).

570 The present study demonstrates that RB in combination with green LEDs has a notable
571 effect on *S. aureus* and *S. Typhimurium* cell viability. RB concentrations and illumination times
572 used in the statistical experimental design for *S. aureus* and *S. Typhimurium* were generally
573 low, proving the effectiveness of aPDT mediated by RB and green LED light against these
574 microorganisms. This large photodynamic efficiency of RB was expected due to its high singlet
575 oxygen quantum yields, with values around 0.79, which is relatively high among
576 photosensitizers (Neckers & Valdes-Aguilera, 1993).

577 Some authors have studied the efficiency of aPDT with RB against several
578 microorganisms (Cahan R, Schwartz R, Langzam Y & Nitzan Y., 2011; Decraene V, Pratten J
579 & Wilson M. 2006; Freire et al., 2014; Gu et al., 2010; Vieira et al., 2018). However, such

580 studies did not involve green LED light, nor did they work with modified PS structures, and
581 work with the RB encapsulated or added to other compounds.

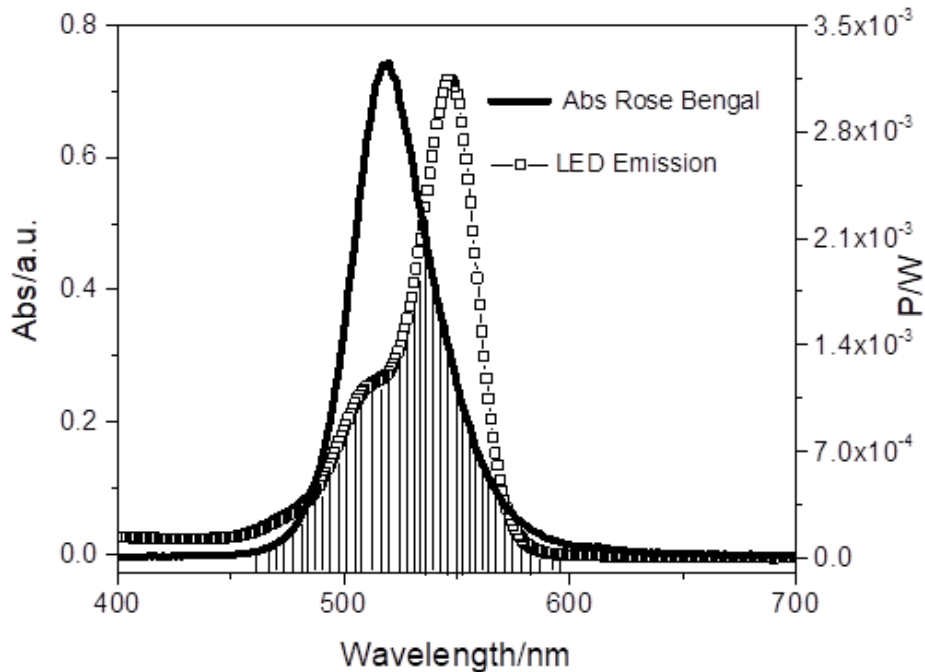
582 Decraene V, Pratten J & Wilson M. (2006), working with a cellulose acetate-based
583 coating incorporated with RB and toluidine blue, at 25 μM for each dye, and using a compact
584 fluorescent light, achieved a reduction in *S. aureus* viability of 2.5 log CFU mL^{-1} and 6.3 log
585 CFU mL^{-1} with lighting times of two and six hours, respectively. Cahan R, Schwartz R,
586 Langzam Y & Nitzan Y. (2011), using RB immobilized on hydrophobic polymers and a white
587 luminescent lamp as light source and illumination time of 24 hours, obtained reductions in *S.*
588 *aureus* viability of approximately 5 log CFU mL^{-1} . Guo Y, Rogelj S & Zhang P. (2010)
589 achieved a reduction in *S. aureus* counts of approximately 6 log CFU mL^{-1} using Rose Bengal-
590 decorated silica nanoparticles at 3 μM and light with a 525 nm filter during 40 minutes (light
591 dose of 33 J cm^{-2}).

592 There are a few studies using RB as PS against *Salmonella* spp. Dahl T, Midden WR &
593 Neckers DC. (1988) obtained a reduction of approximately 90 % in the viability of *S.*
594 *Typhimurium* using RB at 5 μM . However, they used a dark incubation time of 120 minutes
595 and an illumination time of about 80 minutes, with a tungsten filament incandescent lamp.
596 Brovko et al. (2009), using concentrations of RB of 50 and 500 $\mu\text{g mL}^{-1}$, illuminating for 30
597 minutes using a halogen lamp, obtained reductions > 6 Log CFU ml^{-1} in *S. Typhimurium* counts.

598 In our work, with the PS in its conventional form, we obtained better results, even with
599 a lower RB concentration and illumination time than the mentioned studies. These results can
600 be explained by the kind of light source used in our work. It is known that an ideal PS and light
601 source for aPDT should have an appropriate combination of emission and absorption
602 wavelengths (Fracalossi et al., 2016). The use of green LEDs provides a good overlap between
603 the absorbance of the RB and the emission of LED light, which can be observed in our work,

604 where the hatched area in Fig. 7 shows the effectively overlapping between the spectral
 605 irradiance of the green light source and the RB spectral absorption.

606



607

608 Fig. 7 – Light-emitting diode emitted potency (PLED Emitted) and absorbed potency by RB (PAbs). Absorbance
 609 (arbitrary unit); wavelength (nm); potency (Watt) (— Abs Rose Bengal; —□— LED emission).

610

611 Some studies have reported minimal effects of aPDT mediated by xanthene dyes on
 612 Gram-negative bacteria, compared with Gram-positive bacteria (Bonin et al., 2018; Cahan R,
 613 Schwartz R, Langzam Y & Nitzan Y., 2011; Decraene V, Pratten J & Wilson M. 2006;
 614 Yassunaka et al., 2015; Vieira et al., 2018). In our work, we reached total inhibition of *S.*
 615 *Typhimurium*; however, it required a concentration of RB approximately 1000 times greater
 616 than that used for *S. aureus* – this fact could be attributed to differences in the cell wall barrier
 617 properties of these bacteria.

618 The Gram-positive species, such as *S. aureus*, have a porous cell wall that allows
 619 penetration of most PS. Once the PS can penetrate the cell, it damages other targets such as
 620 proteins, enzymes, and DNA (Luksiene & Zukauskas, 2009; Waite & Yousef, 2009). In

621 contrast, Gram-negative bacteria such as *S. Typhimurium* have a cell wall that provides a
622 physical and functional barrier to anionic compounds, such as RB, and hence the PS can be
623 traversed and accumulated slowly (Dahl T, Midden WR & Neckers DC., 1988; Luksiene &
624 Zukauskas, 2009).

625 In this work, RSM was applied to estimate the interaction effects of the PS concentration
626 and illumination time on aPDT of *S. aureus* and *S. Typhimurium*. The application of the RSM
627 showed that the concentration of PS and illumination time are important, but it is necessary to
628 evaluate them separately to reflect their true influence on the response. In this sense, it was
629 possible to observe that *S. aureus* was more susceptible to RB concentration and, that the photo
630 inhibitory action increased in RB in a concentration-dependent manner. In agreement with this
631 result, Manoil D, Filieri A, Schrenzel J & Bouillaguet S. (2016), evaluating *E. faecalis*
632 photoinactivated by RB at 1 μM , 5 μM and 10 μM , and illuminating with a lamp emitting blue-
633 light for 15, 60, and 240 seconds, also observed a greater influence of the RB concentration
634 instead of illumination time.

635 *S. Typhimurium* was more susceptible to illumination time than PS concentration. This
636 result could be related to *S. Typhimurium* cell walls providing a barrier to PS penetration, and,
637 consequently, leading to difficulty in reaching intracellular targets. In this case, it would be
638 necessary to provide more illumination time for the PS to generate singlet oxygen and cause
639 cellular damage. According to Jemli M, Alouini Z, Sabbahi S & Gueddari M. (2002) to improve
640 the efficacy of RB toward Gram-negative bacteria, it is necessary to increase the dye
641 concentration and promote excessive light exposure.

642 Another important fact shown by RSM is that *S. Typhimurium* has its maximum
643 inhibition with approximately 65 μM of RB, and in higher concentrations RB efficiency begins
644 to decrease (Fig. 2B). This result may be related to the effect referred to as self-aggregation,
645 which is commonly observed in xanthene dyes at high concentrations (Xu & Neckers, 1987).

646 It is known that the formation of aggregates affects the ability of a photosensitizer,
647 because it modifies the photophysical properties of the dyes, the absorption spectrum and
648 decreases the quantum yield of singlet oxygen ($\phi_{\Delta 1}O_2$) (Valdes-Aguilera & Neckers, 1989).
649 This result corroborates with the uptake of RB by *S. Typhimurium* which increased until RB at
650 38.00 μM , reduced with RB at 64.20 μM and stabilized, even when RB concentration increased
651 to 75.05 μM .

652 Bacteria exposed to aPDT loses membrane integrity. This loss represents significant
653 damage for cells, once multiple functions are linked to the plasma membrane (Joux & Lebaron,
654 2000; Jiang et al., 2013). With the flow cytometry technique is possible to detect different
655 microbial subpopulations based on the integrity of the membrane, through the retention or
656 exclusion of dyes (Manoil D, Filieri A, Schrenzel J & Bouillaguet S., 2016). Both *S. aureus* and
657 *S. Typhimurium* treated with aPDT showed a high percentage of death or injured cells. The
658 latter showed the simultaneous presence of SYTO-9 and PI in the cells promoted by a partial
659 loss of membrane integrity.

660 The loss of membrane integrity of *S. aureus* and *S. Typhimurium* is consistent with
661 reports from other studies with aPDT (Jiang et al., 2013; Deng et al., 2016; Manoil D, Filieri A,
662 Schrenzel J & Bouillaguet S., 2016; Bonin et al., 2018), as well as with our findings by SEM
663 and TEM. The treated groups showed morphological changes and internal cell structural
664 alterations after photodynamic action. These findings demonstrate that membrane integrity
665 damage may lead to cellular content leakage and can cause cell death.

666 The present study demonstrated that aPDT mediated by RB and green LED light was
667 able to inactivate *S. aureus* and *S. Typhimurium* even at low light doses and PS concentrations.
668 Increased permeability to propidium iodide, as well as morphological and internal cellular
669 alterations after photodynamic action shown by *S. aureus* and *S. Typhimurium* indicate that cell
670 membranes may be an important target of aPDT. The polynomial models developed could

671 provide accurate information on the combined influences of RB concentration and illumination
672 time in aPDT treatment. The RSM showed that, for *S. aureus*, the RB concentration was the
673 variable that most influenced the aPDT treatment, while illumination time had more influence
674 on aPDT for *S. Typhimurium*. Hence, these findings provide important information to be
675 considered in future research with respect to applying aPDT in the food industry.

676

677 **ACKNOWLEDGMENTS**

678 The authors would like to thank the Coordenação de Aperfeiçoamento de Pessoal de Nível Superior -
679 CAPES and the Complexo de Central de Apoio a Pesquisa (COMCAP) of the State University of Maringa.

680

681 **SUPPORTING INFORMATION**

682 Supplementary material associated with this article can be found in the online version.

683

684 **CONFLICT OF INTEREST**

685 No conflict of interest declared.

686

687 **REFERENCES**

688 Al-Asmari F, Mereddy R, Sultanbawa Y. 2018. The effect of photosensitization mediated by curcumin on storage
689 life of fresh date (*Phoenix dactylifera* L.) fruit. *Food Control* 93: 305-309.

690 <https://doi.org/10.1016/j.foodcont.2018.06.005>

691 Anju VT, Paramanatham P, Lal Sruthil SB, Sharan A, Alsaedi MH, Dawoud TMS, Syed A, Siddhardha B. 2018.
692 Antimicrobial photodynamic activity of rose bengal conjugated multi walled carbon nanotubes against planktonic
693 cells and biofilm of *Escherichia coli*. *Photodiagn photodyn*. 24: 200-210. doi:10.1016/j.pdpdt.2018.10.013

694 Bartolomeu M, Reis S, Fontes M, Neves MGPMS, Faustino MAF, Almeida A. 2017. Photodynamic Action against
695 Wastewater Microorganisms and Chemical Pollutants: An Effective Approach with Low Environmental Impact.
696 *Water*. 9(9): 630-646. doi:10.3390/w9090630

697 Bonin E, Santos AR, Silva AF, Ribeiro LH, Favero ME, Campanerut-Sá PAZ, Freitas CF, Caetano W, Hioka N,
698 Mikcha JMG. 2018. Photodynamic inactivation of foodborne bacteria by eosin Y. *J Appl Microbiol*. 124(6): 1617-
699 1628. doi:10.1111/jam.13727

- 700 Brovko LY, Meyer A, Tiwana AS, Chen W, Liu H, Filipe CD, Griffiths MW. 2009. Photodynamic treatment: a
701 novel method for sanitation of food handling and food processing surfaces. *J Food Prot.* 72(5): 1020-1024.
702 doi:10.1111/jam.12622
- 703 Cahan R, Schwartz R, Langzam Y, Nitzan Y. 2011. Light-activated antibacterial surfaces comprise
704 photosensitizers [online]. *Photochem Photobiol.* 87(6): 1379-1386. doi:10.1111/j.1751-1097.2011.00989.x
- 705 CDC, Centers for Disease Control and Prevention (2019, March 16). CDC and Food Safety. Retrieved
706 from <https://www.cdc.gov/foodsafety/cdc-and-food-safety.html>
- 707 Costa AC, Rasteiro VM, Pereira CA, Rossoni RD, Junqueira JC, Jorge AO. 2011. The effects of rose bengal and
708 erythrosine-mediated photodynamic therapy on *Candida albicans*. *Mycoses.* 55(1): 56-63. doi:10.1111/j.1439-
709 0507.2011.02042.x
- 710 Dahl T, Midden WR, Neckers DC. 1988. Comparison of photodynamic action by rose bengal in gram-positive and
711 gram-negative bacteria. *Photochem Photobiol.* 48(5): 607-612. doi:10.1111/j.1751-1097.1988.tb02870.x
- 712 Deng X, Tang S, Wu Q, Tian J, Riley WW, Chen Z. 2016. Inactivation of *Vibrio parahaemolyticus* by
713 antimicrobial photodynamic technology using methylene blue. *J Sci Food Agric.* 96(5): 1601–1608.
714 doi:10.1002/jsfa.7261
- 715 Decraene V, Pratten J, Wilson M. 2006. Cellulose Acetate Containing Toluidine Blue and Rose Bengal Is an
716 Effective Antimicrobial Coating when Exposed to White Light. *Appl Environ Microbiol.* 72(6): 4436-4439.
717 doi:10.1128/AEM.02945-05
- 718 Doria Filho, U. 2001. *Introdução à bioestatística para simples mortais* (3th ed). Rio de Janeiro: Negócio.
- 719 Fadel M, Kassab K. 2011. Evaluation of the Photostability and Photodynamic Efficacy of Rose Bengal Loaded in
720 Multivesicular Liposomes. *Trop J Pharm Res.* 10(3): 289-297. doi:10.4314/tjpr.v10i3.5
- 721 Fracalossi C, Nagata JY, Pelloso DS, Terada RSS, Hioka N, Baesso ML, Sato F, Rosalen PL, Caetano W, Fujimaki
722 M. 2016. Singlet oxygen production by combining erythrosine and halogen light for photodynamic inactivation of
723 *Streptococcus mutans*. *Photodiagn Photodyn Ther.* 15: 17-132. doi:10.1016/j.pdpdt.2016.06.011
- 724 Freire F, Costa AC, Pereira CA, Beltrame Junior M, Junqueira JC, Jorge AO. 2014. Comparison of the effect of
725 rose bengal and eosin Y mediated photodynamic inactivation on planktonic cells and biofilms of *Candida albicans*.
726 *Lasers Med Sci.* 29(3): 949-955. doi:10.1007/s10103-013-1435-x
- 727 Gerola AP, Semensato J, Pelloso DS, Batistela VR, Rabello BR, Hioka N, Caetano W. 2012. Chemical
728 determination of singlet oxygen from photosensitizers illuminated with LED: New calculation methodology
729 considering the influence of photobleaching. *J Photochem Photobiol, A.* 232(15): 14–21.

- 730 doi:10.1016/j.jphotochem.2012.01.018
- 731 Guo Y, Rogelj S, Zhang P. 2010. Rose Bengal-decorated silica nanoparticles as photosensitizers for inactivation
732 of gram-positive bacteria. *Nanotechnology*. 21(6). doi:10.1088/0957-4484/21/6/065102
- 733 Hu J, Lin S, Tan BK, Hamzah SS, Lin Y, Kong Z, Zhang Y, Zheng B, Zeng S. 2018. Photodynamic inactivation
734 of *Burkholderia cepacia* by curcumin in combination with EDTA. *Food Res Int*. 111: 265-271.
735 doi:10.1016/j.foodres.2018.05.042.
- 736 Jiang Y, Leung AW, Wang X, Zhang H, Xu C. 2013. Inactivation of *Staphylococcus aureus* by photodynamic
737 action of hypocrellin B. *Photodiagn Photodyn Ther*. 10(4): 600 - 606. doi:10.1016/j.pdpdt.2013.06.004
- 738 Joux F & Lebaron P. 2000. Use of fluorescent probes to assess physiological functions of bacteria at single-cell
739 level. *Microbes and Infection*. 2(12): 1523–1535. doi:10.1016/S1286-4579(00)01307-1
- 740 Jemli M, Alouini Z, Sabbahi S, Gueddari M. 2002. Destruction of fecal bacteria in wastewater by three
741 photosensitizers. *J. Environ. Monit*. 4(4): 511–516. doi:10.1039/B204637G
- 742 Kim JE, Choi NH, Kang SC. 2007. Anti-listerial properties of garlic shoot juice at growth and morphology of
743 *Listeria monocytogenes*. *Food Control*. 18(10): 1198–1203. doi:10.1016/j.foodcont.2006.07.017
- 744 Liu F, Li Z, Cao B, Wu J, Wang Y, Xue Y, Xu J, Xue C, Tang QJ. 2016. The effect of a novel photodynamic
745 activation method mediated by curcumin on oyster shelf life and quality. *Food Res Int* 87: 204–210.
746 <https://doi.org/10.1016/j.foodres.2016.07.012>
- 747 Lopez-Carballo G, Hernandez-Munoz P, Gavara R & Ocio MJ. 2008. Photoactivated chlorophyllin-based gelatin
748 films and coatings to prevent microbial contamination of food products. *Int J Food Microbiol* 126: 65–70.
749 <https://doi.org/10.1016/j.ijfoodmicro.2008.05.002>
- 750 Luksiene Z & Brovko L. 2013. Antibacterial photosensitization-based treatment for food safety. *Food Eng Rev*.
751 5(4): 185–199. doi:10.1007/s12393-013-9070-7
- 752 Luksiene, Z, Buchovec I, & Paskeviciute E. 2009. Inactivation of food pathogen *Bacillus cereus* by
753 photosensitization in vitro and on the surface of packaging material. *J Appl Microbiol* 107: 2037–2046.
754 doi:10.1111/j.1365-2672.2009.04383.x
- 755 Luksiene Z & Paskeviciute E. 2011. Novel approach to decontaminate food-packaging from pathogens in
756 nonthermal
757 and not chemical way: chlorophyllin-based photosensitization. *J Food Eng* 106: 152–158.
758 10.1016/j.jfoodeng.2011.04.024
- 759 Luksiene Z & Zukauskas A. 2009. Prospects of photosensitization in control of pathogenic and harmful micro-

- 760 organisms. *J Appl Microbiol.* 107(5): 1415-1424. doi:10.1111/j.1365-2672.2009.04341.x
- 761 Manoil D, Filieri A, Schrenzel J, Bouillaguet S. 2016. Rose bengal uptake by *E. faecalis* and *F. nucleatum* and
762 light-mediated antibacterial activity measured by flow cytometry [online]. *J Photochem Photobiol, B.* 162: 258-
763 265. doi:10.1016/j.jphotobiol.2016.06.042
- 764 Marciel L, Mesquita MQ, Ferreira R, Moreira B, Neves MGPMS, Faustino MAF, Almeida A. 2018. An efficient
765 formulation based on cationic porphyrins to photoinactivate *Staphylococcus aureus* and *Escherichia coli*. *Future*
766 *Med Chem.* 10(15):1821-1833. doi:10.4155/fmc-2018-0010
- 767 Martins D, Mesquita MQ, Neves MGGPMS, Faustino MAF, Reis L, Figueira E, Almeida A. 2018.
768 Photoinactivation of *Pseudomonas syringae* pv. *actinidiae* in kiwifruit plants by cationic porphyrins. *Planta.*
769 248(2): 409-421. doi:10.1007/s00425-018-2913-y
- 770 Miller M & Cawthorne A. 2017. *Strengthening surveillance of and response to foodborne diseases: a practical*
771 *manual. Introductory module.* World Health Organization, Geneva.
- 772 Ministério da Saúde. Sistema de Informação de Agravos de Notificação (SINAN). Surtos de Doenças Transmitidas
773 por Alimentos no Brasil Informe 2018 (2019, March 16). Available from
774 [http://portalarquivos2.saude.gov.br/images/pdf/2019/fevereiro/15/Apresenta----o-Surtos-DTA---](http://portalarquivos2.saude.gov.br/images/pdf/2019/fevereiro/15/Apresenta----o-Surtos-DTA---Fevereiro-2019.pdf)
775 [Fevereiro-2019.pdf](http://portalarquivos2.saude.gov.br/images/pdf/2019/fevereiro/15/Apresenta----o-Surtos-DTA---Fevereiro-2019.pdf)
- 776 Neckers DC & Valdes-Aguilera OM. 1993. *Photochemistry of the xanthene dyes.* In: *Advances in Photochemistry.*
777 Edited by Volman D, Hammond GS, Neckers DC. John Wiley & Sons, Inc., New York. pp. 315–394.
- 778 Peloi LS, Soares RR, Biondo CE, Souza VR, Hioka N, Kimura E. 2008. Photodynamic effect of light-emitting
779 diode light on cell growth inhibition induced by methylene blue. *J Biosci.* 33(2): 231-237.
- 780 Penha CB, Bonin E, Silva AF, Hioka N, Zanqueta EB, Nakamura TU, Abreu Filho BA, Campanerut-Sa PAZ,
781 Mikcha JMG. 2017. Photodynamic inactivation of foodborne and food spoilage bacteria by curcumin. *LWT Food*
782 *Sci Technol.* 76(B): 198–202. <https://doi.org/10.1016/j.lwt.2016.07.037>
- 783 Pérez-Laguna V, García-Luque I, Ballestac S, Pérez-Artiaga L, Lampaya-Pérez V, Samper S, Soria-Lozano P,
784 Rezusta A, Gilaberte Y. 2018. Antimicrobial photodynamic activity of Rose Bengal, alone or in combination with
785 Gentamicin, against planktonic and biofilm *Staphylococcus aureus*. *Photodiagn photodyn.* 21: 211-216.
786 doi:10.1016/j.pdpdt.2017.11.012
- 787 Rauf MA, Marzouki N, Körbahti BK. 2008. Photolytic decolorization of Rose Bengal by UV/H₂O₂ and data
788 optimization using response surface method. *J Hazard Mater.* 159(2-3): 602-609.
789 doi:10.1016/j.jhazmat.2008.02.098

- 790 Silva AF, Borges A, Giaouris E, Mikcha JMG, Simões M. 2018. Photodynamic inactivation as an emergente
791 strategy against foodborne pathogenic bacteria in planktonic and sessile states. *Critical Reviews in Microbiol* 44(6):
792 667-684. <https://doi.org/10.1080/1040841X.2018.1491528>
- 793 Silva AF, Borges A, Freitas CF, Hioka N, Mikcha JMG, Simões M. 2018. Antimicrobial Photodynamic
794 Inactivation Mediated by Rose Bengal and Erythrosine Is Effective in the Control of Food-Related Bacteria in
795 Planktonic and Biofilm State. *Molecules*. 23(9): 2228-2246. doi:10.3390/molecules23092288
- 796 Tao R, Zhanga F, Tanga, Q, Xub C, Nid Z, Menga X. 2019. Effects of curcumin-based photodynamic treatment
797 on the storage quality of fresh-cut apples. *Food Chem*. 274: 415-421. doi:10.1016/j.foodchem.2018.08.042
- 798 Valdes-Aguilera O & Neckers DC. 1989. Aggregation phenomena in xanthene dyes. *Acc Chem Res*. 22(5): 171-
799 177. doi:10.1021/ar00161a002
- 800 Vieira C, Gomes ATPC, Mesquita MQ, Moura NMM, Neves MGPMS, Faustino MAF, Almeida A. 2018. An
801 Insight into the Potentiation Effect of Potassium Iodide on aPDT Efficacy. *Front Microbiol*. 19: 2665-2681.
802 doi:10.3389/fmicb.2018.02665
- 803 Xu D & Neckers DC. 1987. Aggregation of rose bengal molecules in solution [online]. *J Photochem Photobiol*
804 A. 40: 361 – 370. doi:10.1016/1010-6030(87)85013-X
- 805 Yassunaka NN, Freitas, CF, Rabello BR, Santos PR, Caetano W, Hioka N, Nakamura TU, Abreu Filho BA,
806 Mikcha JMG. 2015. Photodynamic Inactivation Mediated by Erythrosine and its Derivatives on Foodborne
807 Pathogens and Spoilage Bacteria. *Current Microbiol*. 71(2): 243-251. doi:10.1007/s00284-015-0827-5
- 808 Waite JG & Yousef AE. 2009. Antimicrobial properties of hydroxyxanthenes. *Adv Appl Microbiol*. 69: 79–98.
809 doi:10.1016/S0065-2164(09)69003-1
- 810 Wen X, Zhang X, Szewczyk G, El-Hussein A, Huang Y-Y, Sarna T, Hamblin MR. 2017. Potassium iodide
811 potentiates antimicrobial photodynamic inactivation mediated by rose bengal in vitro and in vivo studies.
812 *Antimicrob Agents Chemother*. 61(7): e00467-17. doi:10.1128/AAC.00467-17.
- 813 Wu J, Mou H, Xue C, Leung AW, Xu C, Tang QJ. 2016. Photodynamic effect of curcumin on *Vibrio*
814 *parahaemolyticus*. *Photodiagn Photodyn Ther* 15: 34–39. 10.1016/j.pdpdt.2016.05.004
- 815 Zhang Q, Chen T, Yang S, Wang X, Guo H. 2013. Response surface methodology to design a selective enrichment
816 broth for rapid detection of *Salmonella spp.* by SYBR Green I real-time PCR. *Appl Microbiol Biotechnol*. 97(9):
817 4149-4158. doi:10.1007/s00253-013-4780-6.
- 818

SUPPORTING INFORMATION

819

820

821 **Response Surface Methodology can be used to predict photoinactivation of**
822 **foodborne pathogens using Rose Bengal excited by 530 nm LED.**

823

824

825 Adriele Rodrigues dos Santos*, Alex Fiori da Silva, Camila Fabiano de Freitas, Marcos Vieira
826 da Silva, Evandro Bona, Celso Vataru Nakamura, Noboru Hioka, Jane Martha Gratton
827 Mikcha.

828

829 *Corresponding Author: Laboratório de microbiologia de alimentos, Departamento de análises
830 clínicas e biomedicina, Universidade Estadual de Maringá, Avenida Colombo, 5790, zona 07,
831 Maringá, 87020-900, PR, Brasil.
832 e-mail: adrielesantos@hotmail.com.

833 Table S1. Analysis of variance for the evaluation of the second-order polynomial model.

Source of variation	<i>Staphylococcus aureus</i>					<i>Salmonella Typhimurium</i>				
	Sum of squares	df	Mean square	F-ratio	p-value	Sum of squares	df	Mean square	F-ratio	p-value
Model	14.3425	3	4.7808	14.6167	0.0013	54.6354	3	18.2118	4.0662	0.0001
Residual	2.6166	8	0.3271			4.8110	8	0.6014		
Lack of fit	2.1833	5	0.4367	3.0232	0.1960	1.9717	5	0.3943	9.0134	0.8161
Pure error	0.4333	3	0.1444			2.8393	3	0.9464		
Total	16.9591	11				59.4465	11			

834 Coefficient of determination (R^2) – *S. aureus* = 0.8483 and *S. Typhimurium* = 0.9191;

835 Adjusted coefficient of determination (R^2_{adj}) – *S. aureus* = 0.7219 and *S. Typhimurium* = 0.8887

836

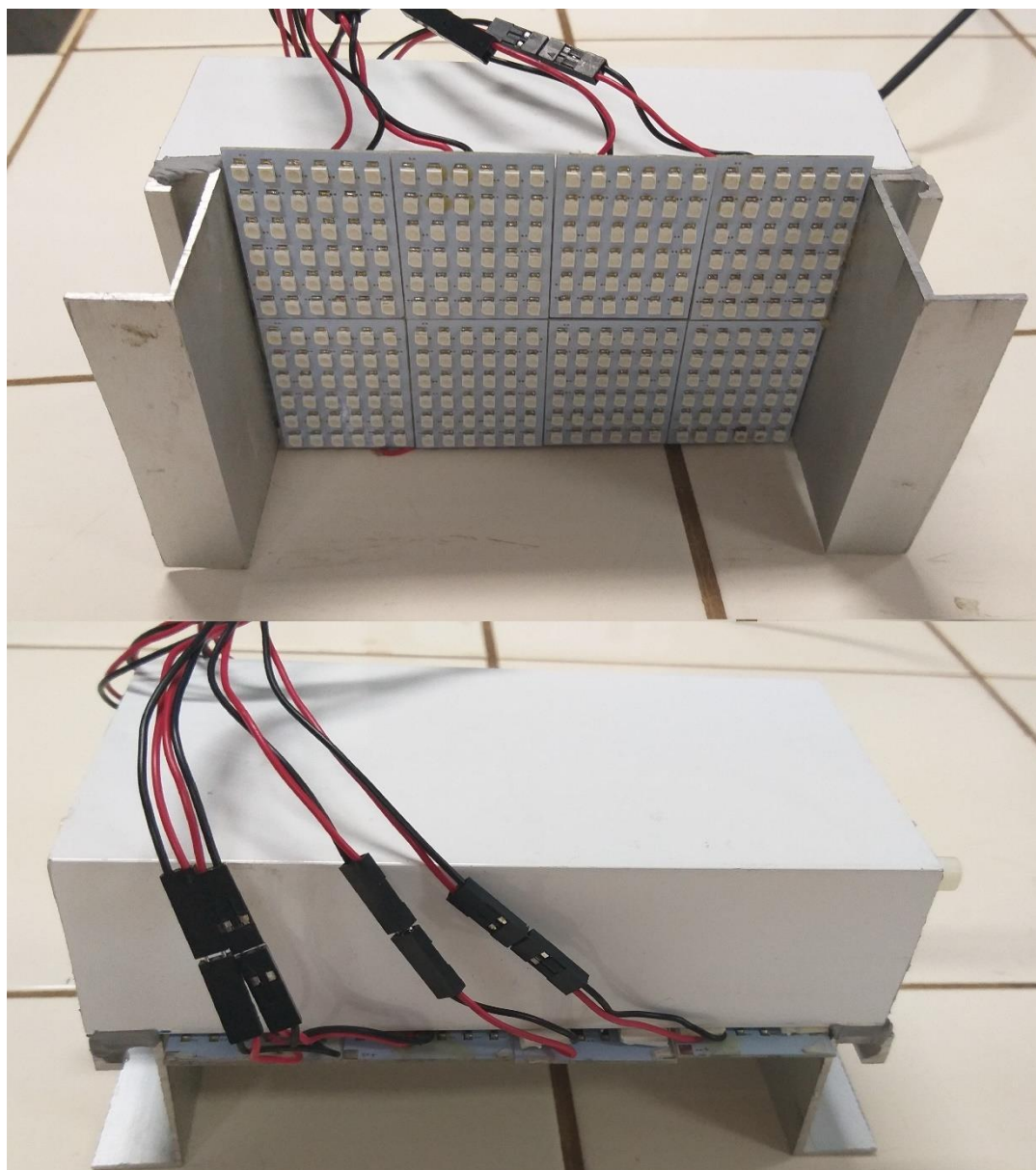
837

838 Table S2. Analysis of variance for the significant terms in the model

Independent variables*	<i>Staphylococcus aureus</i>					<i>Salmonella Typhimurium</i>				
	Sum of squares	df	Mean square	F-ratio	p-value	Sum of squares	df	Mean square	F-ratio	p-value
X ₁	7.0768	1	7.0768	21.6366	0.0016	23.1046	1	23.1046	38.4189	0.0002
X ₁ ²	1.5461	1	1.5461	4.7270	0.0614	5.4992	1	5.4992	9.1442	0.0164
X ₂	5.7194	1	5.7194	17.4864	0.0030	26.0316	1	26.0316	43.2861	0.0001

839 *X₁ – linear effect of PS concentration; X₂ – linear effect of illumination time; X₁² – quadratic effect of PS concentration; X₂².

840 Fig. S1. The homemade prototype of 530 ± 40 nm LED light system.



841



842

843 Article

844 **The Remarkable Effect of Potassium Iodide in**
 845 **Eosin and Rose Bengal Photodynamic Action**
 846 **against *Salmonella* Typhimurium and**
 847 ***Staphylococcus aureus***

848 **Adrielle R. Santos** ^{1*}, **Andréia F. P. Batista** ¹, **Ana T. P. C. Gomes** ², **Maria da Graça P. M. S.**
 849 **Neves** ³,

850 **Maria Amparo F. Faustino** ³, **Adelaide Almeida** ^{2,*}, **Noboru Hioka** ⁴ and **Jane M. G. Mikcha** ^{5*}

851 ¹ Postgraduate Program in Food Science, State University of Maringá, 87020-900 Maringá, Brazil;
 852 andrea.farias04@hotmail.com

853 ² Department of Biology and CESAM, University of Aveiro, 3810-193 Aveiro, Portugal;
 854 ana.peixoto@ua.pt

855 ³ QOPNA& LAQV-REQUIMTE and Department of Chemistry, University of Aveiro, 3810-193 Aveiro,
 856 Portugal; gneves@ua.pt (M.G.P.M.S.N.); faustino@ua.pt (M.A.F.F.)

857 ⁴ Department of Chemistry, State University of Maringá, 87020-900 Maringá, Brazil; nhioka@uem.br

858 ⁵ Department of Clinical Analysis and Biomedicine, State University of Maringá, 87020-900 Maringá,
 859 Brazil

860 * Correspondence: adrielesantos@hotmail.com (A.R.S.); aalmeida@ua.pt (A.A.);
 861 jmgmikcha@uem.br (J.M.G.M.)

862 Received: 17 October 2019; Accepted: 4 November 2019; Published: date

863 **Abstract:** Antimicrobial photodynamic therapy (aPDT) has been shown as a promising
 864 technique to inactivate foodborne bacteria, without inducing the development of bacterial
 865 resistance. Knowing that addition of inorganic salts, such as potassium iodide (KI), can
 866 modulate the photodynamic action of the photosensitizer (PS), we report in this study the
 867 antimicrobial effect of eosin (EOS) and rose bengal (RB) combined with KI against *Salmonella*
 868 *enterica* serovar Typhimurium and *Staphylococcus aureus*. Additionally, the possible
 869 development of bacterial resistance after this combined aPDT protocol was evaluated. The
 870 combination of EOS or RB, at all tested concentrations, with KI at 100 mM, was able to efficiently
 871 inactivate *S. Typhimurium* and *S. aureus*. This combined approach allows a reduction in the PS
 872 concentration up to 1000 times, even against one of the most common foodborne pathogens,
 873 *S. Typhimurium*, a gram-negative bacterium which is not so prone to inactivation with xanthene
 874 dyes when used alone. The photoinactivation of *S. Typhimurium* and *S. aureus* by both
 875 xanthenes with KI did not induce the development of resistance. The low price of the xanthene
 876 dyes, the non-toxic nature of KI, and the possibility of reducing the PS concentration show that
 877 this technology has potential to be easily transposed to the food industry.

878 **Keywords:** xanthene derivatives; photodynamic inactivation; inorganic salt; antimicrobial
 879 resistance; *Salmonella*

880

881 **1. Introduction**

882 The access to safe food is considered as an important requirement to guarantee the quality
883 of human life in modern society [1,2]. In fact, outbreaks of foodborne diseases are one of the main
884 causes of morbidity and mortality being considered as an international public health problem [3],
885 causing significant social and economic impacts [4]. According to the World Health Organization
886 (WHO), it is estimated that more than 600 million people get sick as the result of unsafe food
887 consumption [5,6]. One of the emerging problems related with foodborne bacteria is the increase
888 of antibiotic resistance. It is known that changes in the patterns of food consumption (the
889 preference for fresh and minimally processed foods), alterations in the globalization of the food
890 market, and the emergence of multidrug resistant (MDR) bacteria have turned the control of
891 foodborne diseases into a challenge [7,8]. According to the Centre for Disease Control and
892 Prevention [9], about 400,000 people per year are affected by foodborne infections caused by MDR
893 bacteria in the United States. Multidrug resistant *Salmonella* spp. and *Staphylococcus aureus* are a
894 cause of concern since they have been isolated from meat, poultry, and dairy [10-14].

895 Nowadays, it is assumed that the development of novel antibiotics will not solve the MDR
896 bacteria problem, since microorganisms may find new pathways of resistance to these new
897 molecules. Therefore, efforts should be made towards the development of more efficient, non-
898 toxic, and noninvasive antimicrobial methods to apply to the hosts. Importantly, these new
899 methods should not induce the development of antimicrobial resistance [15-17]. Toward this end,
900 antimicrobial photodynamic therapy (aPDT) has been considered as a promising non-antibiotic
901 approach to inactivate foodborne bacteria [18-23].

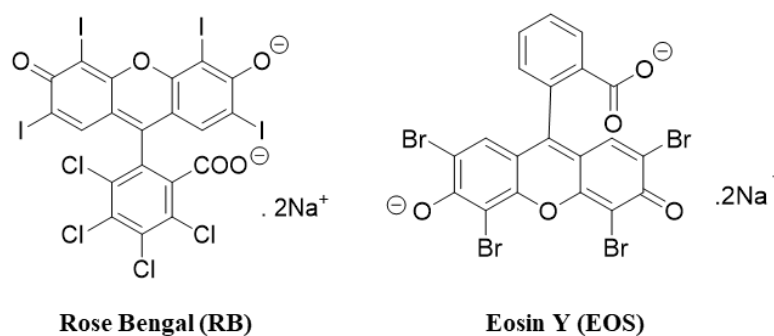
902 aPDT involves the use of a photosensitizer (PS) that when excited by light reacts with
903 molecular oxygen producing reactive oxygen species (ROS) such as singlet oxygen and/or
904 hydroxyl radicals, superoxide, and hydrogen peroxide [15,23]. These ROS can react with
905 biological molecules (e.g., proteins, lipids, and nucleic acids) causing microbial death [16,24,25].
906 This technique presents several advantages when compared with the use of traditional
907 antimicrobials, showing to be efficient independently of the antimicrobial resistance profile and
908 to prevent further development of resistance even after several cycles of treatment [15-17,26]. This
909 approach has been efficient to inactivate several microorganisms, such as gram-negative and
910 gram-positive bacteria [18,19,21], fungi [15,27-29], and viruses [15,30], and to degrade the matrix
911 of microbial biofilms and kill the resident bacteria [16,31,32].

912 An ideal PS is a molecule that is present, in general, with a high quantum yield of singlet
913 oxygen (Φ_{Δ}), low photo-bleaching yield, high affinity for the targeted site, and high stability
914 [33,34]. Xanthene dyes have been considered good PSs to induce bacterial photoinactivation due
915 to their low price, high molar absorptivity, and high singlet oxygen quantum yield (Φ_{Δ}) [18,33,35].
916 The xanthene dyes, rose bengal (RB) and eosin Y (EOS) (Figure 1), have already proven to be
917 effective against gram-positive and gram-negative bacteria [19,20,31,36], however, these dyes
918 showed to be more effective against gram-positive bacteria. This limitation can be overcome by
919 the use of different organic salts such as sodium bromide, sodium azide, sodium thiocyanate, and
920 potassium iodide (KI) [36-38]. Recently, some studies have demonstrated that the combinations
921 of PSs and the inorganic salt KI improve the efficiency of aPDT [15,36,39-41]. Some xanthene dyes
922 are approved for use in drug, cosmetic, and medical applications, and as food additives [19,31],
923 while the safety of KI has been reported by a Food and Drug Administration (FDA) document
924 [42].

925 aPDT certainly is a promising tool to inactivate food and food surfaces. However, to adopt
926 and implement photoinactivation in the food industry, a variety of factors, both those related to
927 aPDT and those related to the food matrix, need to be evaluated [3,43]. Most of the studies with
928 aPDT in food matrices or food-related contamination have been done at laboratory scale, and
929 have focused on fruits, vegetables, and poultry, or food contact surfaces [3,43]. Tao et al. [22]
930 applied different concentrations of curcumin in fresh-cut Fuji apple inoculated with *Escherichia*
931 *coli*. The fruits were illuminated with a 420 nm LEDs on both sides, at a 4 cm distance from the
932 LED. The authors observed a reduction in *E. coli* population, as well in the activity of the enzymes

933 polyphenol oxidase and peroxidase. Aurum and Nguyen [44] achieved a 2 log inactivation of *E.*
 934 *coli* on grapes treated with curcumin at 1.6 μM . The grapes were immersed in curcumin solutions
 935 containing the inoculum for 60 min and the samples were afterwards irradiated with a blue LED
 936 light (465–470 nm). Luksiene and Paskeviciute [45], using Na-Chl at 0.75 μM and a 405 nm LED,
 937 tested the efficacy of PDI against *Listeria monocytogenes* Ly 56 cells attached on polyolefine. They
 938 observed that the aPDI were able to eliminate a 4 log CFU/cm² of bacterial population. The results
 939 of these studies showed that no negative effects were observed in the food matrices [22,44].

940 Therefore, the aim of this work was to investigate the antimicrobial photodynamic effect of
 941 the xanthene dyes RB and EOS combined with the inorganic salt KI against *Salmonella*
 942 Typhimurium and *Staphylococcus aureus*. Additionally, the aim was to evaluate the bacterial
 943 resistance induced by the combination of RB/EOS, KI, and light irradiation.
 944



945

946

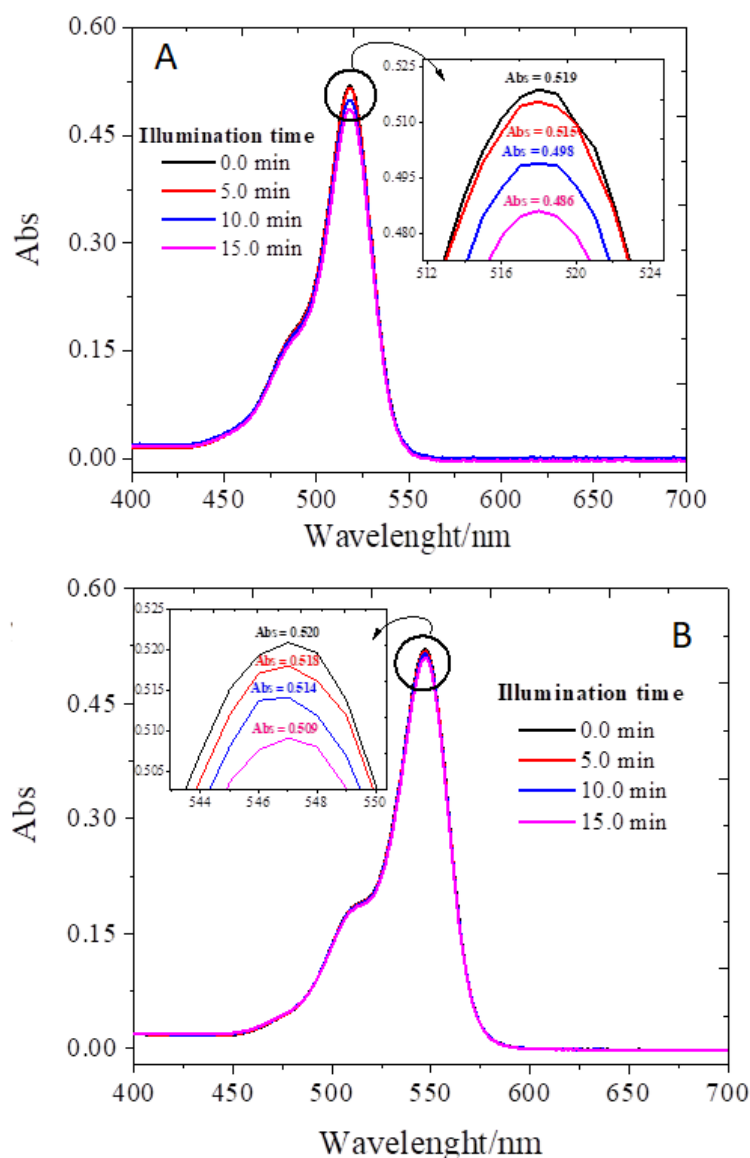
Figure 1. Chemical structures of rose bengal (RB) and eosin Y (EOS).

947

948 2. Results and Discussion

949 2.1. Photostability Assay

950 The absorption spectra of EOS (Figure 2A) and RB (Figure 2B) before and after being
 951 irradiated for 15 min, under the conditions used in the photodynamic assays (vide infra) show a
 952 slight decrease in the maximum absorption intensity (ca 6% and 2%). The decrease is dependent
 953 on the irradiation time and these results are in agreement with the work of Rabello et al. [46],
 954 where it was reported that EOS has a higher tendency to suffer photobleaching than RB. In future
 955 research the absorption spectra of the combined use of xanthenos dyes with KI may be conducted
 956 to better ascertain the use of these PSs in association with green LED light to control bacterial
 957 contamination.



958

959

960

Figure 2. Photobleaching of EOS (**A**) and RB (**B**) without KI in PBS illuminated by a set of LEDs (10 mW/cm² and a wavelength of 530 ± 40 nm) for a period of 0, 5, 10, and 15 min.

961

2.2. Photodynamic Inactivation Assays

962

963

964

965

966

967

968

969

970

971

972

973

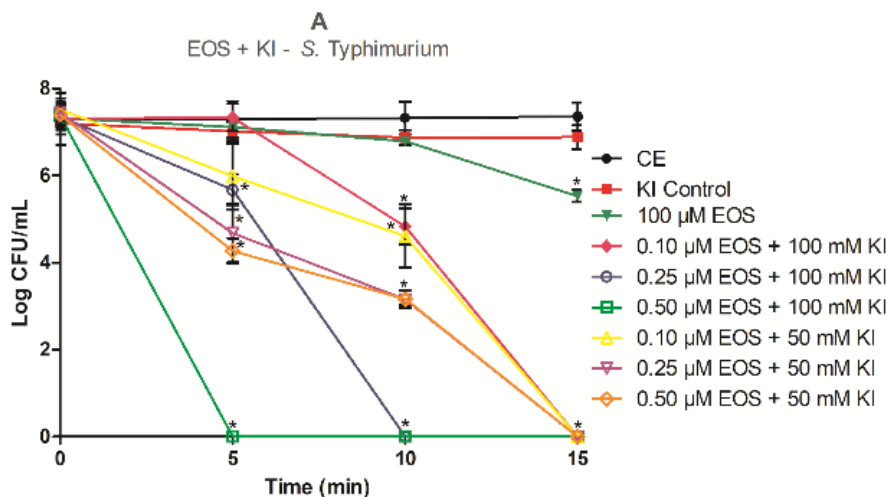
974

975

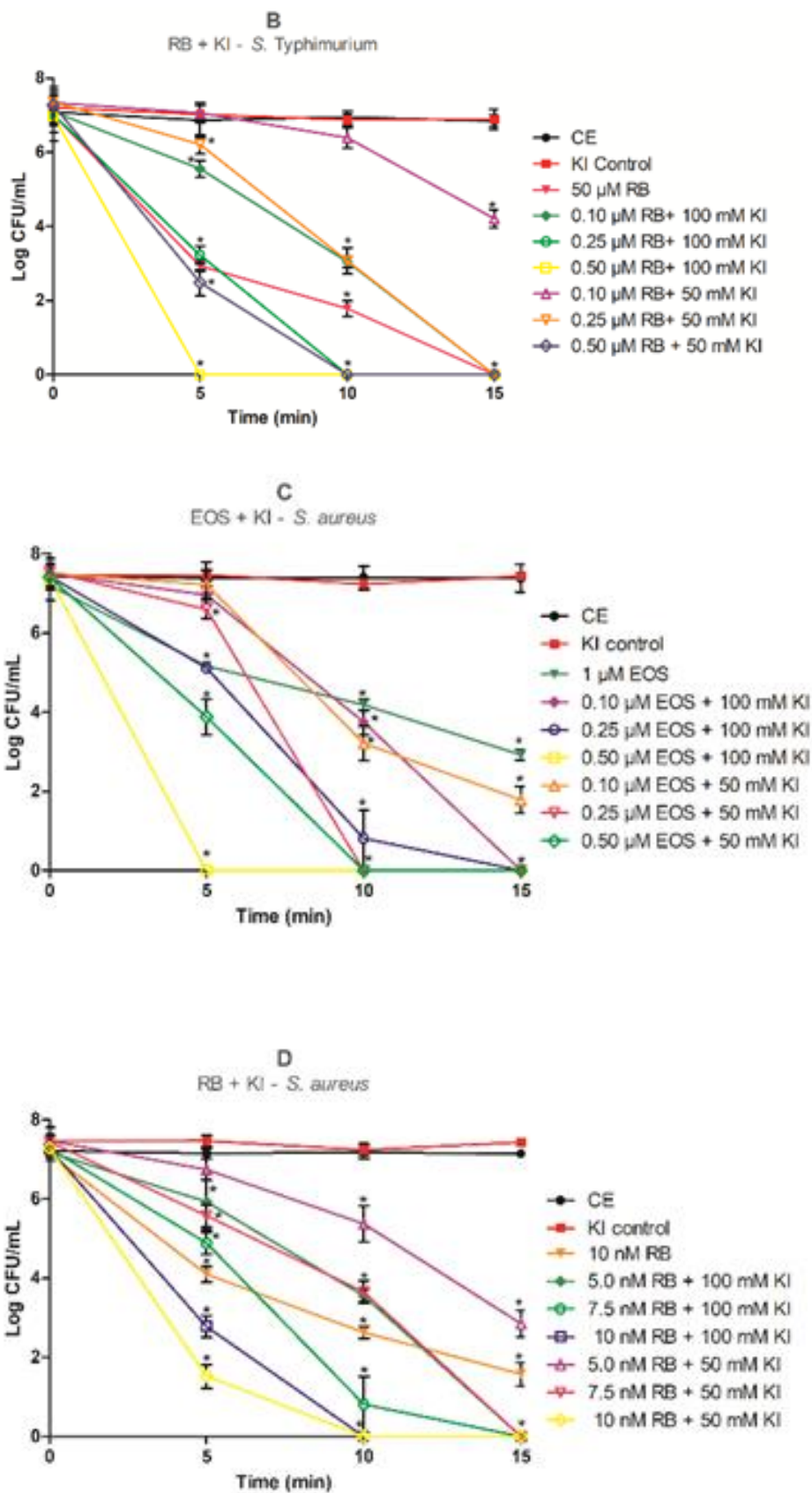
Although the xanthene derivatives dyes RB and EOS, in aqueous buffer solution, show high singlet oxygen quantum yield ($\Phi_{\Delta} = 0.75$ for RB, and $\Phi_{\Delta} = 0.57$ for EOS), which is enough to inactivate gram-positive bacteria, at neutral pH, they are dianionic protolytic molecules [33]. This is a limitation for the photoinactivation of gram-negative bacteria, once they are mostly impermeable to anionic or neutral charged dyes [41]. However, recently Hamblin described an efficient photoinactivation of *E. coli* in the presence of an anionic porphyrin combined with KI [37]. Having this mind, we have decided to study if the photodynamic effect of EOS and RB towards *S. aureus* and *S. Typhimurium* is potentiated by KI. The concentration of RB, EOS, and KI, as well as the irradiation times were chosen based on previous studies of our research group [15,19,31]. So, RB was tested at 10.0 nM alone and, at 5.0 nM, 7.5 nM, and 10 nM combined with KI, for *S. aureus* (a gram-positive bacterium) and at 50 μ M alone and, 0.10 μ M, 0.25 μ M, and 0.50 μ M with KI, for *S. Typhimurium* (a gram-negative bacterium). The concentrations of EOS for the assays in the absence of KI were 1.0 μ M for *S. aureus* and 100 μ M for *S. Typhimurium*. In the presence of KI, the EOS concentrations tested were 0.10 μ M, 0.25 μ M, and 0.50 μ M for both *S.*

976 *aureus* and *S. Typhimurium*. In these assays the KI concentrations used were of 50 mM and 100
 977 mM for both bacteria. The results obtained are presented in Figure 3. The dark control samples
 978 (PSs + KI in the dark (DC)) and the light control (bacteria strains only irradiated with LED (LC))
 979 (data not shown) had no reductions on bacterial population compared with bacterial control
 980 group (bacterium strain only in PBS). The KI control also did not show differences in the *S. aureus*
 981 and *S. Typhimurium* cells reduction when compared with the control group ($p < 0.05$), as shown
 982 in Figure 3A–D.

983 The results obtained for the inactivation of *S. Typhimurium* mediated by EOS and RB alone
 984 show that these PSs have a limited efficacy in the photoinactivation of this gram-negative
 985 bacterium (Figure 3A, B). When EOS was used alone (Figure 3A), even at 100 μM and after an
 986 irradiation period of 15 min (light dose of $9.0 \text{ J}/\text{cm}^2$), the reduction in the survival of *S.*
 987 *Typhimurium* cells was only about 2 log ($p < 0.05$). Bonin et al. [19] has shown that EOS irradiated
 988 for 15 min with green light ($530 \pm 40 \text{ nm}$) promoted a slight reduction of about 1 log in *S.*
 989 *Typhimurium* survival using the EOS at 10 μM . These results show that increasing the
 990 concentration of EOS led to different photoinactivation profiles of *S. Typhimurium* cells. When
 991 RB alone was used (Figure 3B) it was possible to observe the total inactivation of *S. Typhimurium*
 992 cells with a concentration of 50 μM and 15 min of irradiation ($9.0 \text{ J}/\text{cm}^2$). Silva et al. [31] also
 993 achieved the complete inactivation of *S. Typhimurium* cells with a small irradiation time (5 min.),
 994 but they used RB at 75 μM . So, even reaching the inactivation of *S. Typhimurium* cells until the
 995 detection limit of the method with RB, it was necessary for a high concentration of the PS, and
 996 this could be a barrier to its application in the food industry.



997



998

999

1000

1001

1002

1003

Figure 3. Effect of different times of irradiation and concentrations of EOS and RB combined with KI in the inactivation of *Salmonella Typhimurium* (A, B) and *Staphylococcus aureus* (C, D) cells. Samples were incubated in the dark for 10 min and then subjected to 5, 10, or 15 min of green (530 \pm 40 nm) LED light exposure. The control group represents the cells in phosphate-buffered saline

1004 (PBS). Data are presented as mean values and the error bars indicate the standard deviation. * $p <$
1005 0.05. Lines just combine the experimental points.

1006 The combined effect of EOS and RB with KI against *S. Typhimurium* (Figure 3A, B) show
1007 that this combination is effective in the photoinactivation of this gram-negative bacterium. For
1008 the combination 0.10 μM EOS with 100 mM KI total inactivation was observed after 15 min of
1009 irradiation (light dose of 9.0 J/cm^2), while for the combinations 0.25 μM EOS + 100 mM KI and
1010 0.50 μM EOS + 100 mM KI the limit detection of the methodology was achieved after 10 min (6.0
1011 J/cm^2) and 5 min (3.0 J/cm^2) of irradiation, respectively ($p < 0.05$). With the combination EOS + KI
1012 it was possible to completely inactivate the *S. Typhimurium* cells using a PS concentration 1000
1013 times smaller. These data show that KI effectively potentiates EOS in aPDT against this gram-
1014 negative bacterium. For RB, our results also show an aPDT effect surprisingly high, promoting a
1015 reduction in the RB concentration up to 200 times against *S. Typhimurium* (Figure 3B). In this
1016 case it was possible to inactivate *S. Typhimurium* until the detection limit of the method for all
1017 combinations of RB with 100 mM KI as shown in Figure 3B ($p < 0.05$). With the concentration of
1018 RB 0.50 μM with 100 mM KI no culturable cells were recovered even after 5 min of light exposure
1019 (3.0 J/cm^2). In agreement with previous studies [38,39], it was also possible to observe that the
1020 photoinactivation rate increases with the increase of the PS or KI concentration or with the time
1021 of irradiation ($p < 0.05$; Figure 3). Our results are in accordance with Wen et al. [41] and Vieira et
1022 al. [36] that showed a great improvement in the action of the xanthene dye RB against gram-
1023 negative bacteria with the addition of KI.

1024 The use of EOS and RB alone in aPDT treatment against *S. aureus* cells proves to be more
1025 effective than for *S. Typhimurium* (Figure 3C, D). Nevertheless, it was not possible to achieve
1026 complete inactivation of the bacterium cells, even with the longest irradiation time (15 min; 9.0
1027 J/cm^2). On the other hand, Bonin et al. [19] used 5.0 μM of EOS alone to achieve the total inhibition
1028 of the bacterium at 5 min of light exposure. While Silva et al. [20] reported that it was necessary
1029 to use 25 nM RB alone to achieve total inhibition of *S. aureus* cells with the same time of light
1030 exposure (5 min).

1031 Additionally, the combination of EOS and RB with KI also achieved a good improvement in
1032 the photoinactivation action against *S. aureus* (Figure 3C, D). When experiments were performed
1033 with EOS at 0.10 μM and 0.25 μM with 100 mM KI a total inactivation was observed after 15 min
1034 (9.0 J/cm^2) of irradiation. When the concentration of EOS was increased for 0.50 μM no cultivable
1035 cells were recovered after 5 min (3.0 J/cm^2) of irradiation ($p < 0.05$; Figure 3C). Instead, for EOS
1036 alone at 1 μM and 5 min (3.0 J/cm^2) of irradiation, a reduction of about only 2 logs was achieved.
1037 In the photoinactivation mediated by RB with 100 mM KI, the total inactivation of *S. aureus* was
1038 observed for all PS studied concentrations ($p < 0.05$; Figure 3D). When it was used RB at 10 nM
1039 with 100 mM KI the total inactivation of the bacterium cells was achieved with 10 min (6.0 J/cm^2)
1040 of irradiation ($p < 0.05$). While when the RB was used alone, in the same concentration and time
1041 of irradiation, it was observed that it achieved a reduction of about 3 logs in the *S. aureus* cells (p
1042 < 0.05).

1043 In our aPDT studies, namely when KI was used, the necessary PS concentration to inactivate
1044 the bacteria was very low, which probably would not affect the food. However, in a near future,
1045 further experiments, using food matrices, are needed in order to evaluate the potential of this
1046 combined aPDT approach in food industry.

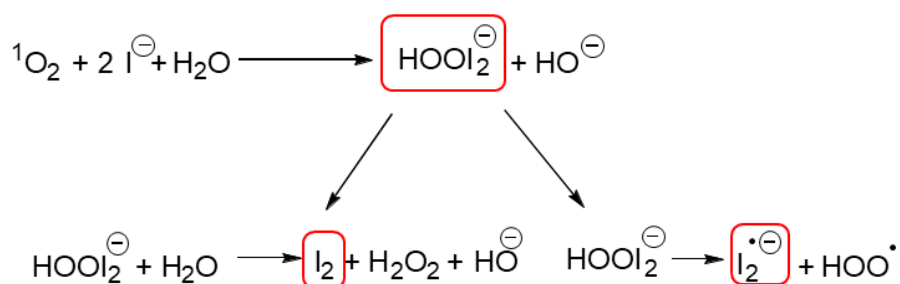
1047 It was possible to observe that the effect of KI was more pronounced when combined with
1048 EOS rather than RB, as expected. According to Huang et al. [47] when a PS already has a
1049 pronounced activity, such as RB, further improvements are more difficult to be achieved. But as
1050 EOS has a lower activity on its own, KI easily improved its photodynamic effect.

1051 Some research groups that studied the use of PSs with KI in aPDT stated that, when a PS is
1052 used in combination with KI, it is necessary to have lower PS concentration or lower light
1053 exposure than when used in non-combined strategies [15,36,38-41,47-49]. The potentiated effect
1054 of RB by KI was studied in the photoinactivation of *E. coli* and *S. aureus* [36,41]. *E. coli* cells exposed

1055 to RB with KI and a light dose of 10 J/cm² (540 ± 15 nm) were reduced in more than 6 logs, while
 1056 when KI was omitted, less than 1 log of killing was found [41]. Vieira et al. [36] also demonstrated
 1057 that RB alone showed no photoinactivation effect in *E. coli* cells, but that the addition of KI
 1058 provided the reduction of the cells until the detection limit of the method was reached.
 1059 Methicillin-resistant *Staphylococcus aureus* (MRSA) was reduced about 2 logs with 100 nM of RB
 1060 alone plus light (20 J/cm²), but when KI (100 mM) was added eradication of cells at 20 J/cm² was
 1061 observed [41]. Importantly, to our knowledge, there are no reports of the combined use of EOS
 1062 with KI against *S. aureus* and *S. Typhimurium*.

1063 Some studies have shown that KI also enhances the effect of other PS classes [36,38-40,47-
 1064 49]. The potentiated effect of KI was observed for porphyrin-based PSs, Photofrin [40] and, for a
 1065 formulation constituted by five cationic porphyrin derivatives [15], in the photoinactivation of
 1066 gram-negative and gram-positive bacteria. The combined effect of MB and KI for the
 1067 photoinactivation of *E. coli* and *S. aureus* was also shown [36,39]. These authors observed that the
 1068 addition of KI increased the bacterial killing in 4 logs for *S. aureus* and 2 logs for *E. coli* [39], as
 1069 well as reduced the time of light exposure of 150 min to 30 min for *E. coli* inactivation [36]. So,
 1070 when comparing our results with these results, we can say that our findings are in line with them.

1071 All the aforementioned studies helped to elucidate how KI acts in the potentiation of aPDT.
 1072 Huang et al. [40] proposed that, for porphyrins, the reaction mechanism occurred via singlet
 1073 oxygen (¹O₂), once they observed an increase of the oxygen consumption when Photofrin was
 1074 irradiated in the presence of KI, as well the generation of hydrogen peroxide. Rose bengal and
 1075 EOS show high singlet oxygen quantum yield and they operate predominantly via the type II
 1076 photochemical pathway, as well as porphyrins. So, for these dyes this extra killing effect of KI is
 1077 caused by several parallel reactions that initiates with the reaction of ¹O₂ with KI [15,36-
 1078 38,40,41,49] (Figure 4). These reactions could produce free iodine (I₂/I₃⁻) and hydrogen peroxide
 1079 (H₂O₂), that are stable species, as well as the short-lived reactive iodine radicals (I₂^{•-}). The stable
 1080 species (I₂/I₃⁻ and H₂O₂) are mostly involved in the photokilling of gram-negative bacteria [37].
 1081 This could be explained because the thin cell wall of gram-negative bacteria allows iodine species
 1082 to penetrate and kill them easier, in comparison with other microbial cells with thicker cell walls
 1083 [41], while the short-lived radicals (I₂^{•-}) were most involved in the photokilling of gram-positive
 1084 bacteria [37].



1085

1086 **Figure 4.** Schematic representation of the decomposition of peroxyiodide into free iodine (I₂/I₃⁻)
 1087 and hydrogen peroxide (H₂O₂) or iodine radicals (I₂^{•-}) (elaborated according with the literature
 1088 [24,37-40,43-45]).

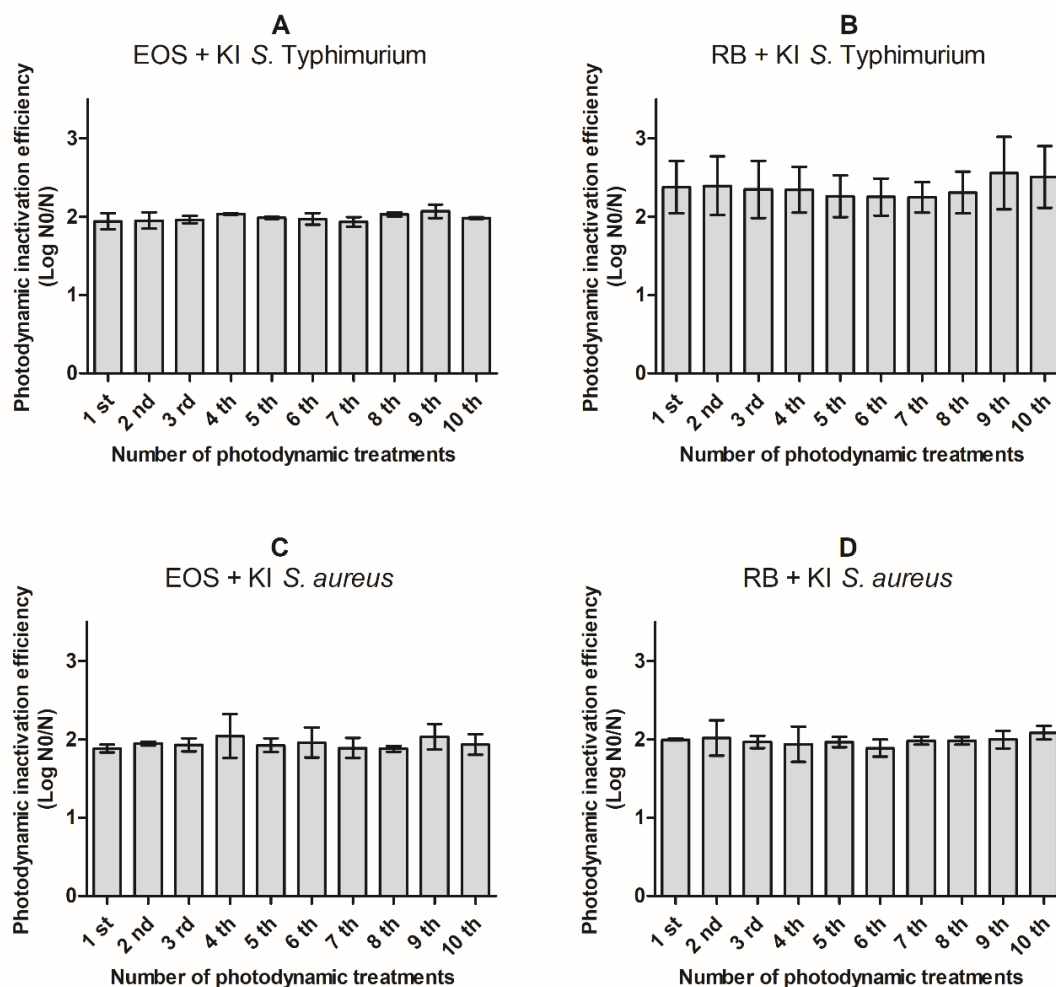
1089 Some authors suggest that free iodine must reach a threshold concentration to be
 1090 microbicidal and that this amount of free iodine produced is directly related to the amount of
 1091 singlet oxygen produced, as well as the concentration of iodide anion present in the solution
 1092 [36,37]. It is believed that due to the very short lifetime of singlet oxygen, the probability of being
 1093 quenched by iodide is higher when the iodide concentration is high, thus the iodide concentration
 1094 is important in aPDT [40].

1095 When we used KI at 50 mM, a half of the usual KI concentration, in combination with EOS
1096 or RB, a strong potentiate effect in the photoinactivation of *S. Typhimurium* and *S. aureus* is still
1097 observed, compared to the PSs alone [19,20] (Figure 3; $p < 0.05$). However, it was possible to
1098 observe that when EOS at 0.50 μM with KI at 50 mM was used, an additional time of light
1099 exposure of 10 min (9.0 J/cm²) are needed, in comparison with the same EOS concentration with
1100 KI at 100 mM, to totally photoinactivate *S. Typhimurium* (Figure 3A). When the EOS
1101 concentration was reduced to 0.10 μM with KI at 50 mM it was not necessary an addition of light
1102 exposure to reach the total photoinactivation of *S. Typhimurium* cells, compared with KI at 100
1103 mM. For the combination of RB at 0.25 μM and 0.50 μM with KI at 50 mM, it was observed that
1104 was necessary to use higher irradiation times to reach the total photokilling of *S. Typhimurium*
1105 cells (>7 log of reduction), compared with the KI at 100 mM (Figure 3B). The assays performed
1106 with the lowest RB concentration (0.10 μM) in the presence of KI at 50 mM showed a reduction
1107 of approximately 3 logs even after an irradiation time of 15 min (total light dose 9.0 J/cm²). Wen
1108 et al. [41] eradicated *E. coli* cells using KI at 25 mM and a light dose of 10 J/cm², however, a RB
1109 concentration 100 times higher was used. These results suggest that if the concentration of KI is
1110 reduced, it is necessary to increase the PSs concentration or the light exposure time to achieve the
1111 same photoinactivation profile.

1112 When EOS at 0.50 μM combined with KI at 50 mM was used against *S. aureus* it was possible
1113 to observe a similar profile, to photoinactivate *S. Typhimurium*; it was necessary to increase the
1114 time of light exposure to achieve total inhibition of the bacterium (Figure 3C). A reduction of
1115 approximately 6 log was achieved when the KI concentration was halved and it was used at the
1116 lowest EOS concentration (0.10 μM) with a light exposure of 15 min (9.0 J/cm²). When we tested
1117 the highest RB concentration (10 nM) in combination with KI at 50 mM, total inactivation of *S.*
1118 *aureus* cells was observed after 10 min of light exposure (Figure 3D). This result was the same
1119 observed for RB at 10 nM but with KI at 100 mM. It is known that the xanthene derivatives weakly
1120 binds to most microorganisms. In this case, some authors suggest that concentrations up to 100
1121 mM of KI are necessary to have an improvement in the PS action [38,40,41]. In our study we really
1122 achieved a great improvement in the PSs' action when KI was used at 100 mM, but for lower KI
1123 concentrations, high inactivation rates was also achieved.

1124 2.3. aPDT Resistance Assays

1125 Actually, multidrug resistant bacteria are one of the most serious health problems in world.
1126 It is known that some multidrug resistant foodborne pathogens have been found in food for
1127 human consumption [7,10-14]. In this sense, aPDT can be a promising alternative once it affects a
1128 high number of microbial targets simultaneously, thus preventing the development of bacterial
1129 resistance [16,36]. In order to evaluate the potential development of bacteria resistance to aPDT
1130 treatment mediated by RB or EOS with KI, ten cycles of photoinactivation under similar
1131 conditions to the ones applied for the photoinactivation profile determination were performed.
1132 Thus, concentration of PS + KI and the irradiation time used were chosen based on the reduction
1133 of ca. 50% in the CFU levels. After each cycle of aPDT, the *S. Typhimurium* or *S. aureus* colonies,
1134 that survived to the performed photoinactivation cycle, were aseptically removed from the TSA
1135 plates and re-suspended in PBS, and then submitted to the same photoinactivation protocol. The
1136 results obtained are presented in Figure 5.



1137

1138 **Figure 5.** Photodynamic inactivation efficiency of ten consecutive cycles of *S. Typhimurium* (up),
 1139 and *S. aureus* (down) by 0.10 μM of eosin (EOS) with 100 mM of KI (A, C), 0.10 μM of rose bengal
 1140 (RB) with 100 mM of KI (B), and 5.0 nM of rose bengal (RB) with 100 mM of KI (D) after 10 min
 1141 of irradiation with green LED light (530 ± 40 nm). N0 represents the plaque counts of bacterial
 1142 cells before the irradiation; N represents the plaque counts after the cycle treatment; error bars
 1143 indicate the standard deviation.

1144 The results showed that there was no significant increase ($p < 0.05$) in resistance of *S.*
 1145 *Typhimurium* to photosensitization after 10 consecutive sessions of 10 min with EOS or RB at
 1146 0.10 μM and KI at 100 mM (Figure 5 A, B). Similar behavior was observed for *S. aureus* cells,
 1147 where no significant increase ($p < 0.05$) was observed in the resistance to photodynamic action
 1148 after 10 aPDT cycles (10 min) with EOS at 0.10 μM or RB at 5 nM and KI at 100 mM (Figure 5 C,
 1149 D). Lauro et al. [50] stated that the development of bacterial resistance could be detected by
 1150 important reductions on the bacterial photoinactivation efficiency among experiments. These
 1151 results clearly show the aPDT protocol with both EOS and RB with KI against *S. Typhimurium*
 1152 and *S. aureus* does not induce development of resistance.

1153 Some studies were conducted to determine if bacterial resistance occurs after several
 1154 consecutive aPDT treatments [16,51]. Tavares et al. [51] also did not observe development of *E.*
 1155 *coli* resistance by 10 cycles of 25 min of irradiation (white light 4.0 mW/cm²) with 5.0 μM of Tri-
 1156 Py⁺-Me-PF. The same conclusions were reported by Bartolomeu et al. [16] working with three
 1157 strains of *S. aureus* treated with Tetra-Py⁺-Me at 5.0 μM and illuminated by white light (4.0
 1158 mW/cm²) by 10 consecutive cycles of aPDT. However, to our knowledge there are no published

1159 results that determine if bacterial resistance occurs when the PS is used in combination with KI
1160 after several consecutive aPDT treatments.

1161 3. Materials and Methods

1162 3.1. Bacterial Strains and Culture Conditions

1163 *Salmonella enterica* serotype Typhimurium (ATCC 14028) and *Staphylococcus aureus* (ATCC
1164 25923) stored at $-20\text{ }^{\circ}\text{C}$ in Brain and Heart Infusion Broth (BHI, Difco, Becton Dickinson, Sparks,
1165 MD, USA) with 20% glycerol, was used in this study. The bacteria were sub cultured in Hektoen
1166 Enteric Agar (Difco, Becton Dickinson, Sparks, MD, USA) for *S. Typhimurium* and Baird Parker
1167 Agar (Difco) for *S. aureus*, and prior to experiments, they were grown overnight at $37\text{ }^{\circ}\text{C}$ in BHI
1168 (Difco, Becton Dickinson, Sparks, MD, USA). Then, the microorganisms were harvested by
1169 centrifugation ($5000\times g$ for 5 min) and washed three times with 0.85% saline solution. The
1170 inoculums were adjusted to approximately 1×10^7 colony-forming units (CFU) per mL and used
1171 in the experiments [20].

1172 3.2. Photosensitizers and LED Light Source

1173 A stock solution of RB and EOS (Sigma Aldrich, Darmstadt, Germany) at 1.0 mM was
1174 prepared in PBS pH 7.2, filter sterilized, standardized in a spectrophotometer (UV-Vis Beckman
1175 Coulter DU *800) and kept in the dark under refrigeration until use [19].

1176 The green LED homemade device prototype has 252 LEDs appropriately arranged on a plate
1177 of 13 cm length \times 8 cm width, with a distance from the microplate surface of 3.5 cm. The prototype
1178 has an irradiance of 10 mW/cm^2 and a wavelength of $530 \pm 40\text{ nm}$. The spectral emission of the
1179 LEDs system was obtained using a spectrofluorimeter (Varian Cary Eclipse, San Diego, CA,
1180 USA). The absolute irradiance of the LEDs was evaluated with a Spectroradiometer
1181 USB2000+RAD (Ocean Optics, Winter Park, FL, USA).

1182 3.3. Photostability Assay

1183 The photostability of EOS and RB was evaluated in PBS. The samples were continuously
1184 illuminated by a set of LEDs (10 mW/cm^2 and a wavelength of $530 \pm 40\text{ nm}$) for a period of 0, 5,
1185 10 and 15 min and the LED system were adapted to the Varian Cary-60 spectrophotometer. This
1186 spectrophotometer works with phase-modulated radiation, allowing the experiment to be
1187 conducted without interference from external radiation. So, 2.0 mL of the aqueous solution
1188 containing the dyes were added in a quartz cuvette (1.0 cm optical pathway). The LED system
1189 was positioned at the top of the cuvette and the spectral reading was initiated using the kinetic
1190 method of the equipment. Finally, the spectral variations were properly evaluated [46].

1191 3.4. Photodynamic Inactivation Assays

1192 The photoinactivation assays were performed according to Silva et al. [20]. In a 24-well plate
1193 $500\text{ }\mu\text{L}$ of bacterial suspension with different concentrations of RB or EOS with KI were kept in
1194 the dark for 10 min to promote the PS + KI binding to bacterial cells before irradiation.
1195 Simultaneously, four control groups were also evaluated: positive control (C), containing only
1196 the bacterial inoculum in PBS without illumination; light control (LC), containing only the
1197 bacterial inoculum in PBS exposed to the same light conditions as the samples; KI control (KIC),
1198 containing the bacterial inoculum in PBS + KI exposed to the same light protocols and; dark
1199 control (DC) containing the inoculum and PS + KI without illumination. After incubation, the
1200 samples, LC and KIC were exposed to the green LED light for 5, 10 and 15 min.

1201 Finally, samples from each well were serially diluted in 0.85% saline solution and plated in
1202 duplicate onto Tryptic Soy Agar (TSA, Difco, Becton Dickinson, Sparks, MD, USA). The plates

1203 were incubated at 37 °C for 24 h and the CFU/mL was counted. Experiments were carried out in
1204 duplicate and repeated three times in independent experiments.

1205 3.5. aPDT Resistance Assays

1206 In order to verify the development of resistance to aPDT treatment with RB with KI and EOS
1207 with KI, ten cycles of photoinactivation under similar conditions were performed. The
1208 concentration of PS + KI and the irradiation time used were chosen based on the reduction of ca.
1209 ~50% in the CFU levels. After each cycle of aPDT, the *S. Typhimurium* or *S. aureus* colonies, that
1210 survived to the previous cycle of photoinactivation, were aseptically removed from the TSA
1211 plates and re-suspended in PBS, and then underwent the same photoinactivation protocol. The
1212 optical density of both bacteria suspension, before each assay, was measured to prevent
1213 differences in the aPDT efficiency. The aPDT efficiency was expressed as $\log N_0/N$, where N_0
1214 and N represent the colony counts before and after the irradiation, respectively. Three
1215 independent assays in duplicate were performed [16].

1216 3.6. Statistical Analysis

1217 Statistical analysis was performed by using one-way ANOVA and the Tukey multiple
1218 comparison test (GraphPad Prism 7.0). The level of statistical significance was set at $p < 0.05$. All
1219 experiments were carried out in duplicate and repeated at least three times in independent
1220 experiments.

1221 4. Conclusions

1222 The present study demonstrated that addition of KI at both concentrations tested (50 mM
1223 and 100 mM) can strongly potentiate the aPDT mediated by the xanthene derivatives EOS and
1224 RB. The use of KI allowed a drastic reduction of the PSs concentration (at least 500 times) and
1225 promoted the inactivation even of the gram-negative bacterium *S. Typhimurium*, a bacterium
1226 which is not so prone to inactivation with xanthene dyes when used alone. It was also confirmed
1227 that *S. Typhimurium* and *S. aureus* did not develop resistance mechanisms when submitted to
1228 consecutive cycles of aPDT protocol in the presence of EOS and RB with KI. Therefore, the
1229 effective inactivation of both bacteria without development of resistance, the low price of the
1230 xanthene dyes, the nontoxic nature of KI and the possibility of greatly reducing the EOS and RB
1231 concentrations allow the development of a very promising alternative to control foodborne
1232 pathogens, forecasting its ease of potential transposition to the food industry.

1233 **Author Contributions:** Conceptualization, A.R.S., M.G.P.M.S.N., M.A.F.F., and A.A.; methodology,
1234 A.T.P.C.G. and A.A.; software, A.R.S.; formal analysis, A.R.S. and A.F.P.B.; resources, N.H.; writing—
1235 original draft preparation, A.R.S.; writing—review and editing, A.T.P.C.G., J.M.G.M., A.A., M.G.P.M.S.N.,
1236 and M.A.F.F.; supervision, J.M.G.M. and A.A.

1237 **Funding:** This research received no external funding.

1238 **Acknowledgments:** The authors would like to thank the Coordenação de Aperfeiçoamento de Pessoal de
1239 Nível Superior—CAPES. Thanks are due to the University of Aveiro and FCT/MEC for the financial support
1240 to QOPNA (FCT UID/QUI/00062/2019), CESAM (UID/AMB/50017/2019) research units and to the project
1241 PREVINE (FCT-PTDC/ASPPES/29576/2017), to FCT/MEC through national funds and the co-funding by the
1242 FEDER-Operational Thematic Program for Competitiveness and Internationalization-COMPETE 2020,
1243 within the PT2020 Partnership Agreement. Thanks are also due to the Portuguese NMR and Mass Networks

1244 **Conflicts of Interest:** The authors declare no conflict of interest.

1245

1246

1247 **References**

- 1248 1. Pereira, R.N.; Vicente, A.A. Environmental impact of novel thermal and non-thermal
1249 technologies in food processing. *Food Res. Int.* **2010**, *43*, 1936–1943,
1250 doi:10.1016/j.foodres.2009.09.013.
- 1251 2. Newell, D.G.; Koopmans, M.; Verhoef, L.; Duizer, E.; Aidara-Kane, A.; Sprong, H.; Opsteegh,
1252 M.; Langelaar, M.; Threlfall, J.; Scheutz, F.; et al. Food-borne diseases—The challenges of 20
1253 years ago still persist while new ones continue to emerge. *Int. J. Food Microbiol.* **2010**, *139*
1254 (Suppl. 1), S3–S15, doi:10.1016/j.ijfoodmicro.2010.01.021.
- 1255 3. Silva, A.F.; Borges, A.; Giaouris, E.; Graton Mikcha, J.M.; Simoes, M. Photodynamic
1256 inactivation as an emergent strategy against foodborne pathogenic bacteria in planktonic
1257 and sessile states. *Crit. Rev. Microbiol.* **2018**, *44*, 667–684, doi:10.1080/1040841x.2018.1491528.
- 1258 4. *European Food Safety Authority*. European Food Safety Authority Food-Borne Zoonotic
1259 Diseases. Available online: [https://www.efsa.europa.eu/en/topics/topic/foodborne-zoonotic-](https://www.efsa.europa.eu/en/topics/topic/foodborne-zoonotic-diseases)
1260 [diseases](https://www.efsa.europa.eu/en/topics/topic/foodborne-zoonotic-diseases) (accessed on September 8, 2019).
- 1261 5. World Health Organization. Food Safety. Available online: [http://www.who.int/en/news-](http://www.who.int/en/news-room/fact-sheets/detail/food-safety)
1262 [room/fact-sheets/detail/food-safety](http://www.who.int/en/news-room/fact-sheets/detail/food-safety) (accessed on September 8, 2019).
- 1263 6. *US Food and Drug Administration*. What You Need to Know About Foodborne Illnesses.
1264 Available online: [https://www.fda.gov/food/consumers/what-you-need-know-about-](https://www.fda.gov/food/consumers/what-you-need-know-about-foodborne-illnesses)
1265 [foodborne-illnesses](https://www.fda.gov/food/consumers/what-you-need-know-about-foodborne-illnesses) (accessed on September 8, 2019).
- 1266 7. Alonso, V.P.P.; Queiroz, M.M.; Gualberto, M.L.; Nascimento, M.S. *Klebsiella pneumoniae*
1267 carbapenemase (KPC), methicillin-resistant *Staphylococcus aureus* (MRSA), and vancomycin-
1268 resistant *Enterococcus* spp. (VRE) in the food production chain and biofilm formation on
1269 abiotic surfaces. *Curr. Opin. Food Sci.* **2019**, *26*, 79–86, doi:10.1016/j.cofs.2019.04.002.
- 1270 8. Nyenje, M.; Ndip, R. The challenges of foodborne pathogens and antimicrobial
1271 chemotherapy: A global perspective. *Afr. J. Microbiol. Res.* **2013**, *7*, 1158–1172,
1272 doi:10.5897/AJMRx12.014.
- 1273 9. Centers for Disease Control and Prevention. Centers for Disease Control and Prevention
1274 Antibiotic/Antimicrobial Resistance (AR/AMR). Available online:
1275 <https://www.cdc.gov/drugresistance/food.html> (accessed on September 8, 2019).
- 1276 10. Zehra, A.; Gulzar, M.; Singh, R.; Kaur, S.; Gill, J.P.S. Prevalence, multidrug resistance and
1277 molecular typing of methicillin-resistant *Staphylococcus aureus* (MRSA) in retail meat from
1278 Punjab, India. *J. Glob. Antimicrob. Resist.* **2019**, *16*, 152–158, doi:10.1016/j.jgar.2018.10.005.
- 1279 11. Tang, Y.; Larsen, J.; Kjeldgaard, J.; Andersen, P.S.; Skov, R.; Ingmer, H. Methicillin-resistant
1280 and-susceptible *Staphylococcus aureus* from retail meat in Denmark. *Int. J. Food Microbiol.*
1281 **2017**, *249*, 72–76, doi:10.1016/j.ijfoodmicro.2017.03.001.
- 1282 12. Thung, T.Y.; Radu, S.; Mahyudin, N.A.; Rukayadi, Y.; Zakaria, Z.; Mazlan, N.; Tan, B.H.; Lee,
1283 E.; Yeoh, S.L.; Chin, Y.Z.; et al. Prevalence, virulence genes and antimicrobial resistance
1284 profiles of *Salmonella* serovars from retail beef in Selangor, Malaysia. *Front. Microbiol.* **2017**,
1285 *8*, 2697, doi:10.3389/fmicb.2017.02697.
- 1286 13. Teramoto, H.; Salaheen, S.; Biswas, D. Contamination of post-harvest poultry products with
1287 multidrug resistant *Staphylococcus aureus* in Maryland-Washington DC metro area. *Food*
1288 *Control* **2016**, *65*, 132–135, doi:10.1016/j.foodcont.2016.01.024.
- 1289 14. Moe, A.Z.; Paulsen, P.; Pichpol, D.; Fries, R.; Irsigler, H.; Baumann, M.P.O.; Oo, K.N.
1290 Prevalence and antimicrobial resistance of *Salmonella* isolates from chicken carcasses in retail
1291 markets in Yangon, Myanmar. *J. Food Protect.* **2017**, *80*, 947–951, doi:10.4315/0362-028x.Jfp-
1292 16-407.
- 1293 15. Vieira, C.; Santos, A.R.; Mesquita, M.Q.; Gomes, A.T.P.C.; Neves, M.G.P.M.S.; Faustino,
1294 M.A.F.; Almeida, A. Advances in aPDT based on the combination of a porphyrinic
1295 formulation with potassium iodide: Effectiveness on bacteria and fungi planktonic/biofilm
1296 forms and viruses. *J. Porphyr. Phthalocyanines* **2019**, *23*, 534–545,
1297 doi:10.1142/s1088424619500408.

- 1298 16. Bartolomeu, M.; Rocha, S.; Cunha, A.; Neves, M.G.P.M.S.; Faustino, M.A.F.; Almeida, A.
1299 Effect of photodynamic therapy on the virulence factors of *Staphylococcus aureus*. *Front.*
1300 *Microbiol.* **2016**, *7*, 267, doi:10.3389/fmicb.2016.00267.
- 1301 17. Tavares, A.; Dias, S.R.; Carvalho, C.M.; Faustino, M.A.F.; Tome, J.P.C.; Neves, M.G.P.M.S.;
1302 Tome, A.C.; Cavaleiro, J.A.S.; Cunha, A.; Gomes, N.C.; et al. Mechanisms of photodynamic
1303 inactivation of a gram-negative recombinant bioluminescent bacterium by cationic
1304 porphyrins. *Photochem. Photobiol. Sci.* **2011**, *10*, 1659–1669, doi:10.1039/c1pp05097d.
- 1305 18. Penha, C.B.; Bonin, E.; da Silva, A.F.; Hioka, N.; Zanqueta, É.B.; Nakamura, T.U.; de Abreu
1306 Filho, B.A.; Campanerut-Sá, P.A.Z.; Mikcha, J.M.G. Photodynamic inactivation of foodborne
1307 and food spoilage bacteria by curcumin. *LWT Food Sci. Technol.* **2017**, *76*, 198–202,
1308 doi:10.1016/j.lwt.2016.07.037.
- 1309 19. Bonin, E.; Santos, A.R.; da Silva, A.F.; Ribeiro, L.H.; Favero, M.E.; Campanerut-Sa, P.A.Z.; de
1310 Freitas, C.F.; Caetano, W.; Hioka, N.; Mikcha, J.M.G. Photodynamic inactivation of
1311 foodborne bacteria by eosin Y. *J. Appl. Microbiol.* **2018**, *124*, 1617–1628, doi:10.1111/jam.13727.
- 1312 20. Silva, A.F.; Santos, A.R.; Trevisan, D.A.C.; Bonin, E.; Freitas, C.F.; Batista, A.F.P.; Hioka, N.;
1313 Simoes, M.; Mikcha, J.M.G. Xanthene dyes and green LED for the inactivation of foodborne
1314 pathogens in planktonic and biofilm states. *Photochem. Photobiol.* **2019**, *95*, 1230–1238,
1315 doi:10.1111/php.13104.
- 1316 21. Yassunaka, N.; de Freitas, C.F.; Rabello, B.R.; Santos, P.R.; Caetano, W.; Hioka, N.;
1317 Nakamura, T.U.; de Abreu Filho, B.A.; Mikcha, J.M.G. Photodynamic inactivation mediated
1318 by erythrosine and its derivatives on foodborne pathogens and spoilage bacteria. *Curr.*
1319 *Microbiol.* **2015**, *71*, 243–251, doi:10.1007/s00284-015-0827-5.
- 1320 22. Tao, R.; Zhang, F.; Tang, Q.-J.; Xu, C.-S.; Ni, Z.-J.; Meng, X.-H. Effects of curcumin-based
1321 photodynamic treatment on the storage quality of fresh-cut apples. *Food Chem.* **2019**, *274*,
1322 415–421, doi:10.1016/j.foodchem.2018.08.042.
- 1323 23. Hu, J.; Lin, S.; Tan, B.K.; Hamzah, S.S.; Lin, Y.; Kong, Z.; Zhang, Y.; Zheng, B.; Zeng, S.
1324 Photodynamic inactivation of *Burkholderia cepacia* by curcumin in combination with EDTA.
1325 *Food Res. Int.* **2018**, *111*, 265–271, doi:10.1016/j.foodres.2018.05.042.
- 1326 24. Alves E., Rodrigues, J.M.M., Faustino M.A.F., Neves M.G.P.M.S., Cavaleiro J.A.S., Lin Z.,
1327 Cunha A., Nadais M.H., Tomé J.P.C., Almeida A. A new insight on nanomagnet-porphyrin
1328 hybrids for photodynamic inactivation of microorganisms. *Dyes Pigments* **2014**, *110*, 110:80-
1329 88, doi:10.1016/j.dyepig.2014.05.016.
- 1330 25. Almeida, A.; Faustino, M.A.F.; Tome, J.P.C. Photodynamic inactivation of bacteria: Finding
1331 the effective targets. *Future Med. Chem.* **2015**, *7*, 1221–1224, doi:10.4155/fmc.15.59.
- 1332 26. Mesquita, M.Q.; Dias, C.J.; Neves, M.G.P.M.S.; Almeida, A.; Faustino, M.A.F. Revisiting
1333 current photoactive materials for antimicrobial photodynamic therapy. *Molecules* **2018**, *23*,
1334 2424, doi:10.3390/molecules23102424.
- 1335 27. Diogo, P.; Mota, M.; Fernandes, C.; Sequeira, D.; Palma, P.; Caramelo, F.; Neves, M.G.P.M.S.;
1336 Faustino, M.A.F.; Goncalves, T.; Santos, J.M. Is the chlorophyll derivative Zn(II)e₆Me a good
1337 photosensitizer to be used in root canal disinfection? *Photodiagn. Photodyn. Ther.* **2018**, *22*,
1338 205–211, doi:10.1016/j.pdpdt.2018.04.009.
- 1339 28. Diogo, P.; Fernandes, C.; Caramelo, F.; Mota, M.; Miranda, I.M.; Faustino, M.A.F.; Neves,
1340 M.G.P.M.S.; Uliana, M.P.; de Oliveira, K.T.; Santos, J.M.; et al. Antimicrobial photodynamic
1341 therapy against endodontic *Enterococcus faecalis* and *Candida albicans* mono and mixed
1342 biofilms in the presence of photosensitizers: A comparative study with classical endodontic
1343 irrigants. *Front. Microbiol.* **2017**, *8*, 498, doi:10.3389/fmicb.2017.00498.
- 1344 29. Beirao, S.; Fernandes, S.; Coelho, J.; Faustino, M.A.F.; Tome, J.P.C.; Neves, M.G.P.M.S.; Tome,
1345 A.C.; Almeida, A.; Cunha, A. Photodynamic inactivation of bacterial and yeast biofilms with
1346 a cationic porphyrin. *Photochem. Photobiol.* **2014**, *90*, 1387–1396, doi:10.1111/php.12331.
- 1347 30. Costa, L.; Tome, J.P.C.; Neves, M.G.P.M.S.; Tome, A.C.; Cavaleiro, J.A.S.; Faustino, M.A.F.;
1348 Cunha, A.; Gomes, N.C.; Almeida, A. Evaluation of resistance development and viability

- 1349 recovery by a non-enveloped virus after repeated cycles of aPDT. *Antivir. Res.* **2011**, *91*, 278–
1350 282, doi:10.1016/j.antiviral.2011.06.007.
- 1351 31. Silva, A.F.; Borges, A.; Freitas, C.F.; Hioka, N.; Mikcha, J.M.G.; Simoes, M. Antimicrobial
1352 photodynamic inactivation mediated by rose bengal and erythrosine is effective in the
1353 control of food-related bacteria in planktonic and biofilm states. *Molecules* **2018**, *23*, 2288,
1354 doi:10.3390/molecules23092288.
- 1355 32. Almeida, J.; Tome, J.P.C.; Neves, M.G.P.M.S.; Tome, A.C.; Cavaleiro, J.A.S.; Cunha, A.; Costa,
1356 L.; Faustino, M.A.F.; Almeida, A. Photodynamic inactivation of multidrug-resistant bacteria
1357 in hospital wastewaters: Influence of residual antibiotics. *Photochem. Photobiol. Sci.* **2014**, *13*,
1358 626–633, doi:10.1039/c3pp50195g.
- 1359 33. de Freitas, C.F.; Pellosi, D.S.; Estevao, B.M.; Calori, I.R.; Tsubone, T.M.; Politi, M.J.; Caetano,
1360 W.; Hioka, N. Nanostructured polymeric micelles carrying xanthene dyes for photodynamic
1361 evaluation. *Photochem. Photobiol.* **2016**, *92*, 790–799, doi:10.1111/php.12645.
- 1362 34. Weijer, R.; Broekgaarden, M.; Kos, M.; van Vught, R.; Rauws, E.A.J.; Breukink, E.; van Gulik,
1363 T.M.; Storm, G.; Heger, M. Enhancing photodynamic therapy of refractory solid cancers:
1364 Combining second-generation photosensitizers with multi-targeted liposomal delivery. *J.*
1365 *Photochem. Photobiol. C* **2015**, *23*, 103–131, doi:10.1016/j.jphotochemrev.2015.05.002.
- 1366 35. Estevão, B.M.; Pellosi, D.S.; de Freitas, C.F.; Vanzin, D.; Franciscato, D.S.; Caetano, W.; Hioka,
1367 N. Interaction of eosin and its ester derivatives with aqueous biomimetic micelles:
1368 Evaluation of photodynamic potentialities. *J. Photochem. Photobiol. A* **2014**, *287*, 30–39,
1369 doi:10.1016/j.jphotochem.2014.04.015.
- 1370 36. Vieira, C.; Gomes, A.T.P.C.; Mesquita, M.Q.; Moura, N.M.M.; Neves, M.G.P.M.S.; Faustino,
1371 M.A.F.; Almeida, A. An insight into the potentiation effect of potassium iodide on aPDT
1372 efficacy. *Front. Microbiol.* **2018**, *9*, 2665, doi:10.3389/fmicb.2018.02665.
- 1373 37. Hamblin, M.R. Potentiation of antimicrobial photodynamic inactivation by inorganic salts.
1374 *Expert Rev. Anti Infect. Ther.* **2017**, *15*, 1059–1069, doi:10.1080/14787210.2017.1397512.
- 1375 38. Huang, L.; El-Hussein, A.; Xuan, W.; Hamblin, M.R. Potentiation by potassium iodide
1376 reveals that the anionic porphyrin TPPS4 is a surprisingly effective photosensitizer for
1377 antimicrobial photodynamic inactivation. *J. Photochem. Photobiol. B* **2018**, *178*, 277–286,
1378 doi:10.1016/j.jphotobiol.2017.10.036.
- 1379 39. Vecchio, D.; Gupta, A.; Huang, L.; Landi, G.; Avci, P.; Rodas, A.; Hamblin, M.R. Bacterial
1380 photodynamic inactivation mediated by methylene blue and red light is enhanced by
1381 synergistic effect of potassium iodide. *Antimicrob. Agents Chemother.* **2015**, *59*, 5203–5212,
1382 doi:10.1128/aac.00019-15.
- 1383 40. Huang, L.; Szewczyk, G.; Sarna, T.; Hamblin, M.R. Potassium iodide potentiates broad-
1384 spectrum antimicrobial photodynamic inactivation using photofrin. *ACS Infect. Dis.* **2017**, *3*,
1385 320–328, doi:10.1021/acscinfecdis.7b00004.
- 1386 41. Wen, X.; Zhang, X.; Szewczyk, G.; El-Hussein, A.; Huang, Y.Y.; Sarna, T.; Hamblin, M.R.
1387 Potassium iodide potentiates antimicrobial photodynamic inactivation mediated by rose
1388 bengal in in vitro and in vivo studies. *Antimicrob. Agents Chemother.* **2017**, *61*, e00467-17,
1389 doi:10.1128/aac.00467-17.
- 1390 42. Food and Drug Administration. *Guidance Potassium Iodide as a Thyroid Blocking Agent in*
1391 *Radiation Emergencies*; Food and Drug Administration: Washington, DC, USA, 2001.
- 1392 43. Ghate, V.S.; Zhou, W.; Yuk, H.G. Perspectives and trends in the application of photodynamic
1393 inactivation for microbiological food safety. *Compr. Rev. Food Sci. Food Saf.* **2019**, *18*, 402–424,
1394 doi:10.1111/1541-4337.
1395 12418.
- 1396 44. Aurum, F.S.; Nguyen, L.T. Efficacy of photoactivated curcumin to decontaminate food
1397 surfaces under blue light emitting diode. *J. Food Process. Eng.* **2019**, *42*, e12988, do:
1398 10.1111/jfpe.12988.

- 1399 45. Luksiene, Z.; Paskeviciute, E. Microbial control of food-related surfaces: Na-Chlorophyllin-
1400 based photosensitization. *J. Photochem. Photobiol. B* **2011**, *105*, 69–74,
1401 doi:10.1016/j.jphotobiol.2011.06.011.
- 1402 46. Rabello, B.R.; Gerola, A.P.; Pellosi, D.S.; Tessaro, A.L.; Aparício, J.L.; Caetano, W.; Hioka, N.
1403 Singlet oxygen dosimetry using uric acid as a chemical probe: Systematic evaluation. *J.*
1404 *Photochem. Photobiol. A* **2012**, *238*, 53–62, doi:10.1016/j.jphotochem.2012.04.012.
- 1405 47. Huang, Y.Y.; Wintner, A.; Seed, P.C.; Brauns, T.; Gelfand, J.A.; Hamblin, M.R. Antimicrobial
1406 photodynamic therapy mediated by methylene blue and potassium iodide to treat urinary
1407 tract infection in a female rat model. *Sci. Rep.* **2018**, *8*, 7257, doi:10.1038/s41598-018-25365-0.
- 1408 48. Huang, Y.-Y.; Choi, H.; Kushida, Y.; Bhayana, B.; Wang, Y.; Hamblin, M.R. Broad-spectrum
1409 antimicrobial effects of photocatalysis using titanium dioxide nanoparticles are strongly
1410 potentiated by addition of potassium iodide. *Antimicrob. Agents Chemother.* **2016**, *60*, 5445–
1411 5453, doi:10.1128/AAC.00980-16.
- 1412 49. Huang, L.; Bhayana, B.; Xuan, W.; Sanchez, R.P.; McCulloch, B.J.; Lalwani, S.; Hamblin, M.R.
1413 Comparison of two functionalized fullerenes for antimicrobial photodynamic inactivation:
1414 Potentiation by potassium iodide and photochemical mechanisms. *J. Photochem. Photobiol. B*
1415 **2018**, *186*, 197–206, doi:10.1016/j.jphotobiol.2018.07.027.
- 1416 50. Lauro, F.M.; Pretto, P.; Covolo, L.; Jori, G.; Bertoloni, G. Photoinactivation of bacterial strains
1417 involved in periodontal diseases sensitized by porphycene-polylysine conjugates. *Photochem.*
1418 *Photobiol. Sci.* **2002**, *1*, 468–470.
- 1419 51. Tavares, A.; Carvalho, C.M.B.; Faustino, M.A.F.; Neves, M.G.P.M.S.; Tomé, J.P.C.; Tomé,
1420 A.C.; Cavaleiro, J.A.S.; Cunha, A.; Gomes, N.C.M.; Alves, E.; et al. Antimicrobial
1421 photodynamic therapy: Study of bacterial recovery viability and potential development of
1422 resistance after treatment. *Mar. Drugs* **2010**, *8*, 91–105, doi:10.3390/md8010091.



© 2019 by the authors. Submitted for possible open access publication under the terms and conditions of the Creative Commons Attribution (CC BY) license (<http://creativecommons.org/licenses/by/4.0/>).

1423

1424

1425